DEUTSCHES ELEKTRONEN – SYNCHROTRON

DESY 93–016
ZU-TH 4/93
IKDA 93/5
February 1993

Rare B-Decays in the Standard Model

A. Ali

Deutsches Elektronen-Synchrotron DESY, Hamburg

C. Greub

Universität Zürich, Switzerland

T. Mannel

Technische Hochschule Darmstadt, THD, Darmstadt

ISSN 0418-9833

NOTKESTRASSE 85 · D-2000 HAMBURG 52

To be sure that your preprints are promptly included in the
HIGH ENERGY PHYSICS INDEX,
send them to (if possible by air mail):

DESY
Bibliothek
Notkestraße 85
W-2000 Hamburg 52
Germany

DESY-IfH
Bibliothek
Platanenallee 6
O-1615 Zeuthen
Germany

DESY 93-016
ZU-TH 4/93
IKDA 93/5
February 1993

ISSN 0418-9833

Rare B-Decays in the Standard Model[1]

A. Ali

Deutsches Elektronen Synchrotron DESY, Hamburg, FRG

C. Greub [2]

Universität Zürich, Zürich, Switzerland

T. Mannel

Technische Hochschule Darmstadt, Darmstadt, FRG

Abstract

We review theoretical work done in studies of the Flavour Changing Neutral Current (FCNC) B-decays in the context of the Standard Model. Making use of the QCD-improved effective Hamiltonian describing the so-called $|\Delta B| = 1$ and $|\Delta B| = 2$, $|\Delta Q| = 0$ transitions, we calculate the rates and differential distributions in a large number of B-decays. The FCNC processes discussed here include the radiative decays $B \to X_s + \gamma$, $B \to X_d + \gamma$, and the semileptonic decays $B \to X_s\, \ell^+\ell^-$, $B \to X_d\, \ell^+\ell^-$, $B \to X_s\, \nu_l\bar{\nu}_l$, and $B \to X_d\, \nu_l\bar{\nu}_l$. We also discuss the inclusive photon energy spectrum calculated from the Charged Current (CC) decays $B \to X_c + \gamma$ and $B \to X_u + \gamma$ and the mentioned FCNC radiative decays. The importance of carrying out measurements of the inclusive photon energy spectrum in B-decays is emphasized. Using phenomenological potential models and the Heavy Quark Effective Theory (HQET) we estimate decay branching ratios in a number of exclusive FCNC B-decays. Purely leptonic and photonic decays $(B_d,\ B_s) \to \ell^+\ell^-$ and $(B_d,\ B_s) \to \gamma\gamma$ are also estimated. The principal interest in the studies of FCNC B-decays lies in their use in determining the parameters of the standard Model, in particular the CKM matrix elements and the top quark mass. The parametric dependence of these and other QCD-specific parameters on the rates and distributions is worked out numerically.

[1] to be published in the Proceedings of the ECFA Workshop on the Physics of a B Meson Factory, Editors: R.Aleksan and A.Ali (1993).

[2] partially supported by Schweizerischer Nationalfonds.

1 INTRODUCTION

We give an overview of the work done on FCNC B-decays in the context of the Standard Model (SM) [1]. Being forbidden by the GIM mechanism at the tree level in SM [2], they are governed by one-loop graphs (penguins and boxes) and hence they are also termed as rare B-decays. These decays, like their counterpart FCNC K-decays, provide information on the properties of the top quark, in particular its mass and the three CKM matrix-elements $(V_{ti}; i = d, s, b)$ [3]. In the SM context, the quantitative determination of the top quark parameters is, therefore, the principal goal of all FCNC decays. We shall concentrate here on the so-called $|\Delta B| = 1$, $\Delta Q = 0$ decays, leading to transitions such as $b \to (s, d) + X$, where $X = g$, γ, $\ell^+\ell^-$, and $\nu\bar{\nu}$. None of these decays have been observed so far, though the present experimental upper limits in some of these decays are rather close to their expected rates in the Standard Model [4]. Deviations from the SM predictions would imply the existence of new physics [5]. This makes their systematic study particularly suitable for future B-physics facilities, such as a B factory.

It should be recalled here that the $|\Delta B| = 2$, $\Delta Q = 0$ FCNC processes in B-physics, inducing the mass mixing in the neutral meson sector B_d^0-$\overline{B_d^0}$ and B_s^0-$\overline{B_s^0}$, have already been measured. Judging from the measured value of the phenomenologically relevant parameter in the B_d^0-$\overline{B_d^0}$ sector, $x_d = (\Delta M/\Gamma)_d = 0.67 \pm 0.10$ [6], and increasing experimental evidence that the mixing in the B_s^0-$\overline{B_s^0}$ sector is substantial, perhaps maximal, the mixing probabilities are anything but rare! In SM, one expects $x_s = O(10)$, which makes its measurements one of the most challenging experimental endeavours. The prospects of x_s-measurements have been recently studied in ref. [7] and will not be discussed here. However, in estimating the rates for some of the rare B-decays , we do take into account the constraints provided by the measurements of x_d and $|\epsilon|$, the CP-violating parameter in K decays. We shall be using the Wolfenstein's parametrization for the CKM matrix [8].

Inclusive rates and final state distributions in FCNC B-decays, as well as their CC counterparts, can be calculated in perturbative QCD, which is the theoretical framework relied upon heavily in this work [9]-[15]. For most distributions, however, one needs additionally information about the B-meson wave function, for which we use phenomenological models constrained by CC B-decays [16,17]. The uncertainties in the various parameters, such as m_t, the QCD-scale μ, the B-meson wavefunction, and the CKM matrix are taken into account in numerical estimates of the decay rates and distributions presented here.

In the second part of this report we estimate the decay rates for a large number of exclusive rare B-decays. These necessarily depend on the hadronic form factors and/or coupling constants. We use two approaches here. First, we make use of vector meson dominance (VMD) in the low mass region ($m_X \leq 1\ GeV$) of the inclusive hadron-mass distributions. This, for example, gives an estimate of the decay rate for $B \to K^* + \gamma$ from the inclusive hadron spectrum in the decays $B \to X_s + \gamma$, assuming K^*-dominance in the threshold region $(m_K + m_\pi) \leq m(X_s) \leq 1.0$ GeV. Likewise, assuming that the decays $B \to X_d + \gamma$ in the mass range $2m_\pi \leq m(X_d) \leq 1.0$ GeV are dominated by the exclusive channel $B \to \rho + \gamma$, gives the branching ratio for this channel. The assumption of vector meson dominance in this mass range is reasonable, since there is plenty of experimental evidence for such dominance from low energy experiments [18] and D-meson semileptonic decays. However, transitions to the lowest lying vector meson states are the only exclusive FCNC decay modes of the B-meson

whose branching ratios can be estimated from the inclusive rates and spectra using VMD. For higher hadron masses (1 GeV $\leq M_X \leq$ 2 GeV) recoiling against the photon or leptons in B decays, there are just too many states contributing to allow a meaningful extraction of decay rate in any given decay channel from the inclusive hadron mass distribution alone.

As the second approach, we use the heavy quark effective theory HQET [19,20] to estimate exclusive rare B-decays. The usefulness of the HQET methods in rare B-decays is at present rather limited. Since rare B-decays involve the so-called heavy to light transitions, reliable relations can be obtained only in the static b-quark limit. For example, one can relate rare B-decays, like $B \to K^* + \gamma$, and the CKM-suppressed CC decays, such as $B \to \rho + \ell\nu_\ell$ [21,22], at a specific kinematic point. There are, however, hardly any data available at present to make quantitative predictions. For first estimates, we treat both the b and s quarks as heavy. This then allows to describe a large number of exclusive rare B-decays and the semileptonic decays of B and D mesons in terms of a single Isgur-Wise form factor [19]. It is, however, to be expected that there will be significant power corrections of $O(\Lambda/m_s)$ and higher orders in such relations. Since these corrections have yet to be calculated, the results presented for exclusive rare decays are at best semi-quantitative. On the same issue, rare B-decay rate estimates involve extrapolations of the Isgur-Wise functions in the momentum space much beyond their presently constrained regions. This, in particular, is true for the decays $B \to K^* + \gamma$ and $B \to \rho + \gamma$, making their decay rates vulnerable to parametrizations. We estimate the variations in rates in a number of parametrizations of the Isgur-Wise functions. Predictions for exclusive rare B-decays can be firmed considerably when data on the CKM-suppressed CC B-decays become available.

This report is organized as follows: In section 2, we discuss the inclusive radiative rare B-decays, $B \to X_s + \gamma$ and $B \to X_d + \gamma$ in the Standard Model, where the rates for the latter are obtained by constraining the CKM- matrix element, $|V_{td}|$. We also review estimates of the inclusive energy-momentum profile of the final states in radiative B-decays, including both the FCNC and and CC decays. In particular, measurements of the inclusive photon energy spectrum in B-decays have the potential of determining a number of CKM-matrix elements, which we quantify. In section 3, we discuss the inclusive FCNC semileptonic decays $b \to (s,d) + \ell^+\ell^-$ ($\ell = e, \mu, \tau$) and $b \to (s,d) + \nu\bar{\nu}$. The use of of QCD for these decays is restricted to the evaluation of the improved Wilson coefficients for the relevant operators. Fixing the long distance contribution in the process $B \to X_s\, \ell^+\ell^-$ from data, we discuss the inclusive dilepton invariant mass distribution in the process $B \to X_s\, \ell^+\ell^-$ and the asymmetry in the angular distribution of the $\ell^\pm$ in the dilepton rest frame. The short distance contributions in these distributions are sensitive to the top quark mass [10,23,24] and we show this dependence here. In section 4, we describe some applications of HQET in selected exclusive rare B-decays [25,26]. These include the decays $B \to (K^*, K^{**}) + \gamma$, where K^{**} stands for higher resonances of the K^* series, and the FCNC semileptonic decays $B \to (K, K^*)\ \ell^+\ell^-$ and $B \to (K, K^*)\ \nu_\ell\bar{\nu}_\ell$ [25]. Constraining the CKM-matrix element from the present phenomenology, we give estimates for the corresponding CKM-suppressed decays $B \to (\pi, \rho)\ \ell^+\ell^-$ and $B \to (\pi, \rho)\ \nu_\ell\bar{\nu}_\ell$ [27]. Purely leptonic and photonic decays $(B_d, B_s) \to \ell^+\ell^-$ and $(B_d, B_s) \to \gamma\gamma$ are also given in this section, where we correct a factor 2 reported in the published literature [28,4]. A brief outlook is given in section 5, where the present experimental limits on rare B-decays are also listed.

2 Inclusive radiative B-decays

In estimates of the inclusive radiative decays $B \to X + \gamma$, both the charged current CC radiative transitions $B \to (X_c, X_u) + \gamma$ and the flavour changing neutral current FCNC processes $B \to (X_s, X_d) + \gamma$ have to be taken into account. Here and in what follows the subscript q in X_q denotes the quark transition $b \to q$. The former decays are sensitive to the CKM matrix elements $|V_{cb}|$ and $|V_{ub}|$. On the other hand, the FCNC radiative decays $B \to (X_s, X_d) + \gamma$, induced by the electromagnetic penguins, are essentially determined by the magnetic moment operators, whose Wilson coefficients are dominated by the top quark contribution in the processes $b \to (s,d) + \gamma + (g)$. The rates for these processes therefore depend on the top quark mass m_t and the CKM matrix elements $|V_{ts}|$ (for $B \to X_s + \gamma$) and $|V_{td}|$ (for $B \to X_d + \gamma$) [13]. It follows that a precise measurement of the prompt photon energy spectra in B-decays has, in principle, the potential of determining the four CKM matrix elements: $|V_{cb}|, |V_{ub}|, |V_{ts}|$, and $|V_{td}|$. The main point of this chapter is to stress that one can clearly disentangle the FCNC processes from the CC contributions from measurements of the photon energy spectrum in B-decays. We now discuss the FCNC- and CC-processes separately.

2.1 FCNC processes $B \to X_s\, \gamma$ and $B \to X_d\, \gamma$

The calculations for the FCNC B-decays have been done within the framework of an effective Hamiltonian [10]. The operator basis for the effective Hamiltonian, responsible for the decay under consideration, consists of four-quark operators and the magnetic moment type operators of dimension 6. Operators of higher dimension are suppressed by powers of the masses of the heavy particles (W-boson and top quark) which have been integrated out, and hence are not considered here. First, we give the complete set of operators relevant for the processes $b \to d\gamma, d\gamma g$:

$$H_{eff}(b \to d) = -\frac{4G_F}{\sqrt{2}}\, \xi_t \sum_{j=1}^{8} C_j(\mu)\, O_j(\mu) \quad . \tag{1}$$

Here G_F is the Fermi coupling constant and $\xi_i = V_{ib}\, V_{id}^*$ for $i = t, c, u$. As discussed in refs. [13,14], the dominant contributions arise from the operators O_1, O_2, O_7 and O_8, whereas the operators $O_3, ..., O_6$ get coefficients through operator mixing only, which numerically are negligible. The dominant operators read as follows:

$$\begin{aligned}
O_1 &= -\frac{\xi_c}{\xi_t}(\bar{c}_{L\beta}\gamma^\mu b_{L\alpha})(\bar{d}_{L\alpha}\gamma_\mu c_{L\beta}) - \frac{\xi_u}{\xi_t}(\bar{u}_{L\beta}\gamma^\mu b_{L\alpha})(\bar{d}_{L\alpha}\gamma_\mu u_{L\beta}) \\
O_2 &= -\frac{\xi_c}{\xi_t}(\bar{c}_{L\alpha}\gamma^\mu b_{L\alpha})(\bar{d}_{L\beta}\gamma_\mu c_{L\beta}) - \frac{\xi_u}{\xi_t}(\bar{u}_{L\alpha}\gamma^\mu b_{L\alpha})(\bar{d}_{L\beta}\gamma_\mu u_{L\beta}) \\
O_7 &= (e/16\,\pi^2)\, \bar{d}_\alpha\, \sigma^{\mu\nu}\, (m_b R + m_s L) b_\alpha\, F_{\mu\nu} \\
O_8 &= (g_s/16\,\pi^2)\, \bar{d}_\alpha\, \sigma^{\mu\nu}\, (m_b R + m_s L)\, T^A_{\alpha\beta}\, b_\beta\, G^A_{\mu\nu}
\end{aligned} \tag{2}$$

Here e and g_s denote the QED and QCD coupling constants, respectively, and $L = (1 - \gamma_5)/2$; $R = (1 + \gamma_5)/2$. The effects of QCD corrections, contained in the Wilson coefficients $C_j(\mu)$, have been evaluated to leading logarithmic accuracy. At the renormalization scale μ, which will be varied in numerical evaluations between $(m_b/2)$ and $(2m_b)$, the

dominant coefficients read as follows [10]:

$$
\begin{aligned}
C_1(\mu) &= \frac{1}{2}\left[\eta^{-6/23} - \eta^{12/23}\right] C_2(m_W) \qquad C_2(\mu) = \frac{1}{2}\left[\eta^{-6/23} + \eta^{12/23}\right] C_2(m_W) \\
C_7(\mu) &= \eta^{-16/23}\left\{C_7(m_W) - \frac{58}{135}\left[\eta^{10/23} - 1\right] C_2(m_W) - \frac{29}{189}\left[\eta^{28/23} - 1\right] C_2(m_W)\right\} \\
C_8(\mu) &= \eta^{-14/23}\left\{C_8(m_W) - \frac{11}{144}\left[\eta^{8/23} - 1\right] C_2(m_W) + \frac{35}{234}\left[\eta^{26/23} - 1\right] C_2(m_W)\right\}
\end{aligned}
\tag{3}
$$

with $\eta = \frac{\alpha_s(\mu)}{\alpha_s(m_W)}$. At the scale $\mu = m_W$, where the matching conditions are imposed [29], we have:

$$
\begin{aligned}
C_1(m_W) &= 0 \qquad C_2(m_W) = 1 \\
C_7(m_W) &= \frac{x}{24(x-1)^4}\left[6x(3x-2)\log x - (x-1)(8x^2+5x-7)\right] \\
C_8(m_W) &= -\frac{x}{8(x-1)^4}\left[6x\log x + (x-1)(x^2-5x-2)\right]
\end{aligned}
\tag{4}
$$

with $x = m_t^2/m_W^2$. We note that all the CKM-angle dependent quantities ξ_i $(i = t, c, u)$ in Eq. (1) are of the same order of magnitude. However, in the decays $b \to s\gamma$ and $b \to s\gamma g$ the quantities ξ_i are replaced by $\lambda_i = V_{ib}V_{is}^*$. As $\lambda_u \ll \lambda_t, \lambda_c$, we can neglect λ_u. In this case the CKM matrix dependence in the effective Hamiltonian factorizes completely due to unitarity:

$$
H_{eff}(b \to s) = -\frac{4G_F}{\sqrt{2}}\lambda_t \sum_{j=1}^{8} C_j(\mu)\,\hat{O}_j(\mu) \tag{5}
$$

with

$$
\hat{O}_1 = (\bar{c}_{L\beta}\gamma^\mu b_{L\alpha})(\bar{s}_{L\alpha}\gamma_\mu c_{L\beta}) \qquad \hat{O}_2 = (\bar{c}_{L\alpha}\gamma^\mu b_{L\alpha})(\bar{s}_{L\beta}\gamma_\mu c_{L\beta}) \tag{6}
$$

The remaining operators $\hat{O}_j$ are obtained from the corresponding O_j operators by simply replacing the d field by an s field. Furthermore, the Wilson coefficients in $H_{eff}(b \to s)$ and $H_{eff}(b \to d)$ are identical.

2.1.1 Branching ratios for $B \to X_s + \gamma$ and $B \to X_d + \gamma$

To get the branching ratios and the differential spectra for $B \to X_s + \gamma$ and $B \to X_d + \gamma$, the diagrams associated with the operators O_1, O_2, O_7, and O_8 have to be evaluated. As they are given in refs. [13,14] we do not display them here. It turns out that the diagrams associated with O_1 vanish due to the colour structure. Futhermore, the coefficient of the operator O_8 gets suppressed after including QCD effects and its contribution is neglected. The following results are therefore based on the contributions associated with the operators O_2 and O_7. Omitting the technical details of their evaluation, which may be found in ref. [13], we now discuss the dependence of the branching ratios $B \to X_s + \gamma$ and $B \to X_d + \gamma$ on the various input parameters. The default values of the parameters used in the numerical estimates for the CC and FCNC branching ratios and energy spectra are given in Table 1. We note that we have set $|V_{ts}| = |V_{cb}|$, which follows from the Wolfenstein's parametrization where $|V_{ts}| = |V_{cb}| = A\lambda^2$. Note also, that the assumed value for these coupling constants translates

Parameter	Default value
$m_t\ (GeV)$	140
$m_b\ (GeV)$	5
$m_c\ (GeV)$	1.68
$m_s\ (GeV)$	0.50
$m_u = m_d\ (GeV)$	0.30
$\mu\ (GeV)$	5.0
$\Lambda^{(5)}\ (GeV)$	0.225
$p_F\ (GeV)$	0.3
$\lvert V_{ts}\rvert$	0.044
$\lvert V_{cb}\rvert$	0.044
$\lvert V_{ub}\rvert/\lvert V_{cb}\rvert$	0.08
$\lvert V_{cd}\rvert = \lvert V_{us}\rvert$	0.220
$\lvert V_{cs}\rvert = \lvert V_{ud}\rvert$	0.975

Table 1: List of parameters and their default values used in the numerical estimates of the B-decay rates and photon energy spectra.

into $A = 0.905$, with the PDG value $\lambda = 0.2205$ [18]. Since the masses of the light quarks, m_u, m_d and m_s are numerically not important, we fix them to their default values given in Table 1. The contribution of the charm quark enters through the loop in the diagrams for the decays $b \to (s, d) + \gamma + g$. The decay rates are again not very sensitive to the precise value of m_c, but we shall include the effect of its variation in the range $1.3\ GeV \leq m_c \leq 1.7\ GeV$. The branching ratios are being calculated by using the total B decay width, Γ_{tot}:

$$
\begin{aligned}
\Gamma_{tot} &= \left(r_u\,|V_{ub}|^2 + r_c\,|V_{cb}|^2\right)\Gamma_0 \\
\Gamma_0 &= \frac{m_b^5\,G_F^2}{192\pi^3} \quad ; \quad r_u \approx 7 \quad ; \quad r_c \approx 3
\end{aligned}
\tag{7}
$$

The values of r_u and r_c include phase space and QCD corrections [30,31]. The dependence on the b-quark mass cancels to a very large extent in the branching ratios. We vary m_t in the presently favoured range from the electroweak phenomenology $m_t = 140 \pm 40\ GeV$ [32]. For the scale dependence of the strong coupling constant, which is needed for the estimates of the rates and spectra for the FCNC decays $B \to (X_s, X_d) + \gamma$, we use the two loop β function:

$$
\alpha_s(\mu) = \frac{12\,\pi}{(33 - 2\,N_f)\,\log(\mu^2/\Lambda^2)}\left(1 - \frac{6\,(153 - 19N_f)}{(33 - 2N_f)^2}\,\frac{\log\log(\mu^2/\Lambda^2)}{\log(\mu^2/\Lambda^2)}\right) \tag{8}
$$

We set $N_f = 5$ and the corresponding $\Lambda^{(5)} = 225$ MeV, which is the central value obtained from a recent compilation [33]. It should be remarked here that since the anomalous dimension matrix for rare B decays, used in estimating the rates below, has been evaluated at the 1-loop level, also for the β-funcion we could restrict ourselves to the first term in Eq. (8). However, recent calculations of the anomalous dimension matrix in the effective weak Hamiltonian by Buras et al. [34] show that the anomalous dimensions are not significantly renormalized going from 1-loop to 2-loop. Hence, using the two-loop β function incorporates the bulk of the 2-loop effects in the decay rates. The dependence of the branching ratio $BR(B \to X_s + \gamma)$

on m_t and μ is shown in Fig. 1, where it is plotted as a function of μ with the upper curve corresponding to $m_t = 180\ GeV$ and the lower to $m_t = 100\ GeV$. Based on this figure, a

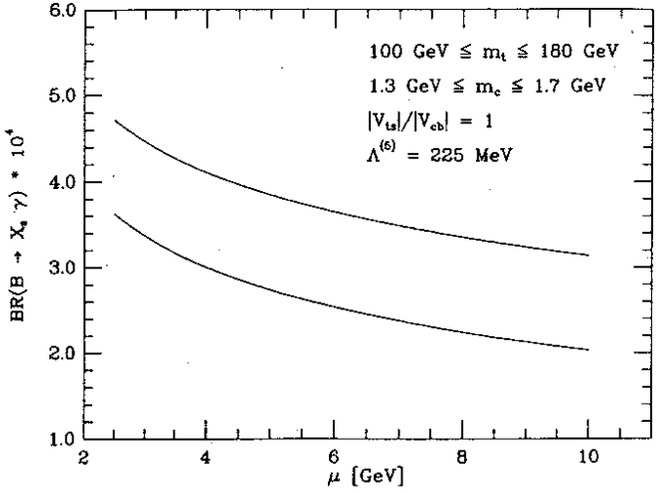

Figure 1: Dependence of the branching ratio for $B \to X_s + \gamma$ on the scale μ and m_t

firm prediction for this branching ratio in the SM is:

$$BR(B \to X_s + \gamma) = (2 - 5) \times 10^{-4} \tag{9}$$

As can be seen in Fig. 1, the m_t-dependence of $BR(B \to X_s + \gamma)$ in the assumed m_t-range is only $O(25\%)$. It would, therefore, be difficult to extract a meaningful bound on m_t from a measurement of $BR(B \to X_s + \gamma)$. We remark that the central value in Fig. 1, $BR(B \to X_s + \gamma) = 3.5 \times 10^{-4}$ (corresponding to $\mu = 5.0\ GeV$ and $m_t = 150\ GeV$), is not too far away from the present bound on this branching ratio, namely $BR(B \to X_s + \gamma) < 8.4 \times 10^{-4}$ (@ 90% $C.L.$) [35]; hence a measurement in this channel is expected soon.

Whereas in the branching ratio for $B \to X_s + \gamma$ the CKM matrix dependence was contained in an overall factor $|\lambda_t|^2$, this is no longer true in the case of $B \to X_d + \gamma$, which we want to discuss now. The nontrivial dependence comes in through the contribution of the operator O_2 in list (1). The dependence of the branching ratio can be written explicitly as:

$$BR(B \to X_d + \gamma) = D_1 |\xi_t|^2 \left\{ 1 - \frac{1-\rho}{(1-\rho)^2 + \eta^2} D_2 - \frac{\eta}{(1-\rho)^2 + \eta^2} D_3 + \frac{D_4}{(1-\rho)^2 + \eta^2} \right\} . \tag{10}$$

Here we have expressed ξ_t and ξ_c in terms of the Wolfenstein parameters A, λ, ρ and η:

$$\begin{aligned} \xi_t &= A\lambda^3(1 - \rho + i\eta) \\ \xi_c &= -A\lambda^3 \end{aligned} \tag{11}$$

The m_t-dependence of the coefficients D_i is rather weak, as shown in Table 2. To get the

$m_t(GeV)$	D_1	D_2	D_3	D_4
100	0.16	0.21	0.04	0.14
120	0.17	0.20	0.04	0.13
140	0.19	0.18	0.04	0.12
160	0.20	0.17	0.04	0.11
180	0.21	0.17	0.03	0.10
200	0.22	0.16	0.03	0.10

Table 2: Values of the coefficients D_i entering in Eq. 10 as a function of m_t.

inclusive branching ratio as a function of m_t, we vary the CKM parameters ρ and η over the presently allowed range. For this purpose we use the following experimental inputs:

$$\left| \frac{V_{ub}}{V_{cb}} \right| = 0.08 \pm 0.02 \tag{12}$$

$$|\epsilon| = (2.26 \pm 0.02) \times 10^{-3} \tag{13}$$

$$x_d = 0.67 \pm 0.10 \tag{14}$$

We use the following expressions for the CP-violating parameter in K-decays $|\epsilon|$, [36]:

$$\begin{aligned} |\epsilon| &= \frac{G_F^2 f_K^2 m_K m_W^2}{6\sqrt{2}\pi^2 \Delta m_K} B_K \left(A^2\lambda^6 \eta \right) \{ x_c \left(\eta_{ct} f_3(x_c, x_t) - \eta_{cc} \right) \\ &\quad + \eta_{tt}\, x_t\, f_2(x_t)\, A^2\lambda^4(1-\rho) \} \end{aligned} \tag{15}$$

Here, the η_i are QCD correction factors, $\eta_{cc} \simeq 0.85$, $\eta_{tt} \simeq 0.61$, $\eta_{ct} \simeq 0.36$ for $\Lambda_{QCD} = 200$ MeV, [37], $m_K = 498$ MeV, $\Delta m_K = 3.5 \cdot 10^{-12}$ MeV, $f_K = 160$ MeV, $x_i \equiv m_i^2/M_W^2$, and the functions f_2 and f_3 are given by

$$\begin{aligned} f_2(x) &= \frac{1}{4} + \frac{9}{4}\frac{1}{(1-x)} - \frac{3}{2}\frac{1}{(1-x)^2} - \frac{3}{2}\frac{x^2 \ln x}{(1-x)^3} \\ f_3(x,y) &= \ln\frac{y}{x} - \frac{3y}{4(1-y)} \left(1 + \frac{y}{1-y} \ln y \right) . \end{aligned} \tag{16}$$

The final parameter in the expression for $|\epsilon|$ is B_K, which represents our ignorance of the matrix element $\langle K^0 | (\bar{d}\gamma^\mu(1-\gamma_5)s)^2 | \overline{K^0} \rangle$. We shall take $B_K = 0.8 \pm 0.2$. This leads to the two hyperbolae in Fig. 2.

We now turn to B_d^0-$\overline{B_d^0}$ mixing parameter x_d, whose value in SM is dominantly determined by the t-quark exchange:

$$x_d \equiv \frac{(\Delta m)_B}{\Gamma} = \tau_B \frac{G_F^2}{6\pi^2} m_W^2 m_B \left(f_{B_d}^2 B_{B_d} \right) \eta_B x_t f_2(x_t) |\xi_t|^2 . \tag{17}$$

Here η_B is the QCD correction factor, for which it was customary to take the leading order result $\eta_B = 0.85$ [36]. There now exists a next-to-leading order calculation for η_B, giving an appreciably lower value, $\eta_B = 0.55$ [38]. It has been stressed in [34] that other parameters remaining the same, the renormalization of η_B has a significant effect in restricting the allowed

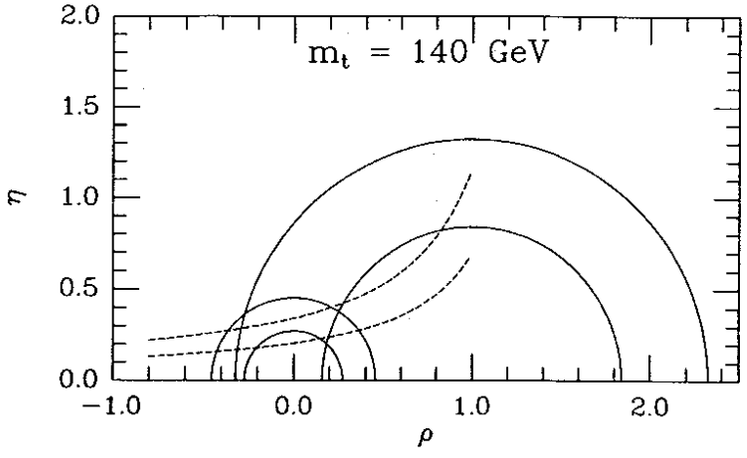

Figure 2: Presently allowed range of the Wolfenstein parameters ρ and η as function of m_t.

(ρ,η) values. In accordance with the recommendations of [34] we set $\eta_B = 0.55$, and assume $f_B\sqrt{B_B} = (0.20 \pm 0.03)$GeV, as suggested by recent Lattice simulations [39]. In addition, we use $\tau_B = 1.36 \times 10^{-12}$ sec, corresponding to the recently updated world average including LEP results [40], and $m_B = 5.277$ GeV [18]. The constraint from x_d leads to two semi-circles centered at $(\rho,\eta) = (1,0)$ shown in Fig. 2.

The resulting branching ratio $BR(B \to X_d + \gamma)$ is shown in Fig. 3 as a function of m_t, from which we predict

$$BR(B \to X_d + \gamma) = (0.8 - 3.2) \times 10^{-5} \tag{18}$$

for the top quark mass in the range $100\,GeV \leq m_t \leq 200\,GeV$. We remark that the μ-dependence of the branching ratio $BR(B \to X_d + \gamma)$ is very significant, which can again be traced to the very significant QCD renormalization of the Wilson coefficients $C_i(m_W) \to C_i(\mu)$, in particular C_7.

2.1.2 Photon energy spectra in FCNC B-decays

Concerning the photon energy spectra in the decays $b \to (s,d) + \gamma + g$, it is to be noted that they have a nonintegrable infrared singularity for $E_g \to 0$, showing up as $E_\gamma \to E_\gamma^{max}$. Adding the contributions of the processes $b \to (s,d)+\gamma+g$ with their respective virtual QCD corrections, the singularity cancels in a distribution sense [13,14]. The end-point spectra, however, show sensitivity to the leftover effects of the (cancelled) infrared singularity, with the photon-energy distribution $\frac{d\Gamma}{dx_\gamma}$ rising very steeply near the end-point, $x_\gamma \simeq 1$ (here x_γ is the fractional energy of the photon, $x_\gamma = E_\gamma/E_\gamma^{max}$). To remedy this we performed a resummation of the leading (infrared) logarithms as discussed in refs. [13,14]. Furthermore, the motion of the b quark in the B meson has to be taken into account. The model incorporating this Fermi motion of the b-quark has previously been used in the derivation of the inclusive lepton energy spectrum in the semileptonic decays of the B and D hadrons [16,17], where it is known to give a good description of the measured lepton energy spectra. In this model the b-quark

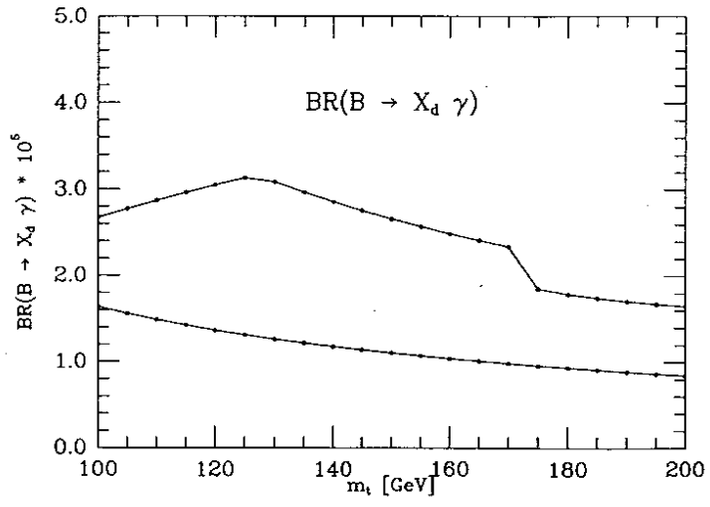

Figure 3: Branching ratio for $B \to X_d + \gamma$ as a function of m_t by varying over the allowed range in the (ρ,η)-plane.

is given a non-zero momentum having a Gaussian distribution represented by an a priori free (but adjustable) parameter, p_F:

$$\phi(p) = \frac{4}{\sqrt{\pi}{p_F}^3}\exp(\frac{-p^2}{{p_F}^2}) \quad ; \quad p = |\vec{p}| \tag{19}$$

The energy-momentum constraint is imposed in the form:

$$W^2 = {m_B}^2 + {m_q}^2 - 2m_B\sqrt{p^2 + {m_q}^2} \tag{20}$$

where m_B is the B-meson mass, W, the effective momentum dependent mass of the b-quark, and m_q, the constant mass of the spectator quark in the B-meson, $B = \bar{b}q$. The detailed formulae for the photon energy spectrum containing the Fermi motion are given in refs. [13, 14]. For p_F, we take the best value obtained from a fit of the ARGUS and CLEO inclusive lepton energy spectrum, $p_F = 0.30 \pm 0.09\ GeV$ [41,42]. The dependence of the inclusive branching ratios for both $B \to X_d + \gamma$ and $B \to X_s + \gamma$ on the wave-function parameter, p_F, is negligible, if one replaces the mass of the b quark in the total decay width (7) by an effective value W_{eff}, which depends on p_F:

$${W^2_{eff}} \simeq {m_B}^2 - 2m_B \cdot p_F \cdot 1.28 \tag{21}$$

However, the shape of the photon energy spectra and the distributions of the invariant mass of the final state hadrons are sensitive to its value, as illustrated in Fig. 4, where we plot the distribution $d\Gamma/dM_X$, for different values of p_F. The photon energy spectra for $B \to X_s + \gamma$ and $B \to X_d + \gamma$ are contained in Fig. 5, using the central value $p_F = 0.30$ GeV. More detailed information may also be found in refs. [13,14,15].

2.1.3 Estimates of $BR(B \to K^* + \gamma)$ and $BR(B \to \rho + \gamma)$

Having the hadronic invariant mass distributions for the decays $B \to X_d + \gamma$ and $B \to X_s + \gamma$, one could attempt to estimate the exclusive branching ratios using the assumption

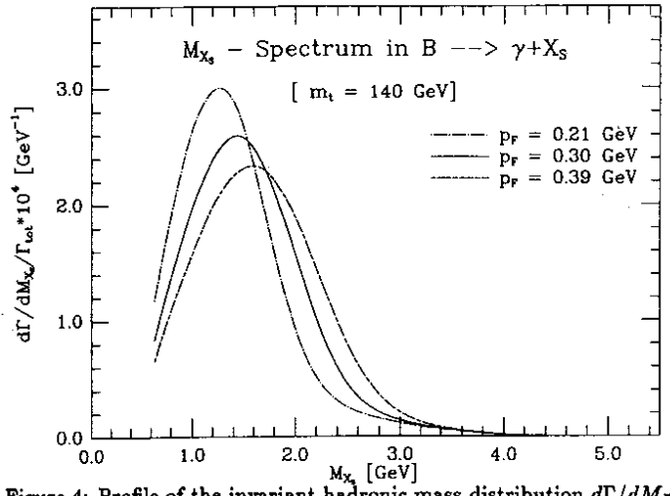

Figure 4: Profile of the invariant hadronic mass distribution $d\Gamma/dM_{X_s}$

of vector meson dominance in the low-mass part of the invariant hadron mass spectrum. The motivation of doing this comes from experimental studies in semileptonic D-decays, in which the hadronic mass spectrum in the range $m_K + m_\pi \leq m_{X_s} \leq 1.0$ GeV is found to be completely saturated by the K^*-resonance. It may therefore be reasonable to assume that in the mass range between $(m_K + m_\pi)$ and 1.0 GeV, the decay $B \to X_s + \gamma$ will be dominated by the K^*-resonance. For the $B \to X_d + \gamma$ case we assume a corresponding saturation by the ρ-resonance in the interval between $(2m_\pi)$ and 1.0 GeV. Following this argument, we integrate the spectra in the decays $B \to X_s + \gamma$ and $B \to X_d + \gamma$ in the ranges

$$m_K + m_\pi \leq M_{X_s} \leq 1\,\text{GeV} \quad \text{and} \quad 2m_\pi \leq M_{X_d} \leq 1\,\text{GeV} \quad , \tag{22}$$

to estimate the branching ratio for $B \to K^* + \gamma$ and $B \to \rho + \gamma$, respectively. The branching ratio for $B \to K^* + \gamma$ is shown in Table 3 for different values of m_t and p_F. To focus attention to this branching ratio, which probably will be the first to be measured in the class of FCNC decays being calculated here, we note that the central values of the parameters ($m_t = 150$ GeV and $p_F = 0.30$ GeV) give:

$$BR(B \to K^* + \gamma) = 5.0 \times 10^{-5}. \tag{23}$$

The branching ratio for $B \to \rho + \gamma$ is shown in Table 4, where the entries again correspond

$m_t(GeV) =$	100	150	200
$p_F = 0.21\ GeV$	5.4	6.8	7.8
$p_F = 0.30\ GeV$	3.9	5.0	5.7
$p_F = 0.39\ GeV$	3.1	4.0	4.5

Table 3: Branching ratio for the decay $B \to K^* + \gamma$ in units of 10^{-5}

to a central values in Fig. 2, namely $(\rho, \eta) = (0.1, 0.3)$. It turns out that to a precision better

$m_t(GeV) =$	100	150	200
$p_F = 0.21\ GeV$	3.6	4.5	5.2
$p_F = 0.30\ GeV$	2.7	3.5	3.9
$p_F = 0.39\ GeV$	2.2	2.8	3.2

Table 4: Branching ratio for the decay $B \to \rho + \gamma$ in units of $10^{-6} \times (|V_{td}|^2/(8.43 \cdot 10^{-5}))$

than 1% this branching ratio depends on ρ and η only through the combination $|\xi_t|^2/|V_{bc}|^2 = \lambda^2[(1-\rho)^2 + \eta^2]$. The reason for this is not too difficult to understand: in the region close to the end-point photon energy spectrum, $E_\gamma \to E_\gamma^{max}$, the magnetic moment operator O_7 dominates and it only depends on $|\xi_t|$, as can be seen from the effective Hamiltonian for $b \to d + \gamma + (g)$. We estimate:

$$BR(B \to \rho + \gamma) = (2.2 - 5.2) \times 10^{-6} \times \left(\frac{|V_{td}|^2}{8.43 \times 10^{-5}} \right) \quad , \tag{24}$$

taking into account the uncertainties in our model (in particular, dependence on p_F and the QCD-scale μ) and with m_t in the range $100\ GeV < m_t < 200\ GeV$. A much firm prediction is however obtained on the relative branching ratios for the decays $B \to \rho + \gamma$ and $B \to K^* + \gamma$:

$$\frac{\Gamma(B \to \rho + \gamma)}{\Gamma(B \to K^* + \gamma)} = (0.07) \times \left(\frac{|V_{td}|^2}{8.43 \times 10^{-5}} \right) \tag{25}$$

The (remaining) m_t and p_F dependence in this ratio is negligible. With the estimate for the branching ratio $BR(B \to K^* + \gamma) = (3 - 8) \times 10^{-5}$ calculated in ref. [13,14], and the present experimental bound $BR(B \to K^* + \gamma) < 9.2 \times 10^{-5}$ (90% $C.L.$) [43], it is fair to conclude that the discovery of this channel is just around the corner. The dependence of the branching ratios $B \to K^* + \gamma$ and $B \to \rho + \gamma$ on the renormalization scale μ follows that of the inclusive branching ratios. This dependence can be as large as 50 % in the individual branching ratios, it tends to cancel in the quantity $BR(B \to \rho + \gamma)/BR(B \to K^* + \gamma)$, however. It should be remarked here that the numerical coefficient in the above relation is specific to our model. In general, it will depend on SU(3)-breaking in the magnetic moment form factors, which, however, we don't expect to be overwhelming. So, in our opinion, Eq. (25) is a pretty firm prediction.

2.2 CC radiative processes $B \to X_c\gamma$ and $B \to X_u\gamma$

The CC radiative decays $B \to X_c + \gamma$ and $B \to X_u + \gamma$ are modelled after the quark decays given in Table 5, where we have also listed the CKM-matrix element dependence of the partial widths through the factor K_n with $n = 1, ..., 14$. They represent single photon bremsstrahlung processes from all the charged fermion lines (leptons and quarks) evaluated in the spectator model. Note that we have neglected the so-called W-exchange two-body decays, since they are generally considered negligible in B-decays [30]. The most convincing experimental support in favour of the dominance of the spectator model contribution is the (near) equality of the charged- and neutral B-meson lifetimes, gotten indirectly through the

n	reaction	K_n
1	$b \to c\, d\bar{u}\gamma$	$3\,\lvert V_{cb}\rvert^2\,\lvert V_{ud}\rvert^2$
2	$b \to c\, d\bar{c}\gamma$	$3\,\lvert V_{cb}\rvert^2\,\lvert V_{cd}\rvert^2$
3	$b \to c\, s\bar{u}\gamma$	$3\,\lvert V_{cb}\rvert^2\,\lvert V_{us}\rvert^2$
4	$b \to c\, s\bar{c}\gamma$	$3\,\lvert V_{cb}\rvert^2\,\lvert V_{cs}\rvert^2$
5	$b \to c\, e^-\bar{\nu}\gamma$	$\lvert V_{cb}\rvert^2$
6	$b \to c\, \mu^-\bar{\nu}\gamma$	$\lvert V_{cb}\rvert^2$
7	$b \to c\, \tau^-\bar{\nu}\gamma$	$\lvert V_{cb}\rvert^2$
8	$b \to u\, d\bar{u}\gamma$	$3\,\lvert V_{ub}\rvert^2\,\lvert V_{ud}\rvert^2$
9	$b \to u\, d\bar{c}\gamma$	$3\,\lvert V_{ub}\rvert^2\,\lvert V_{cd}\rvert^2$
10	$b \to u\, s\bar{u}\gamma$	$3\,\lvert V_{ub}\rvert^2\,\lvert V_{us}\rvert^2$
11	$b \to u\, s\bar{c}\gamma$	$3\,\lvert V_{ub}\rvert^2\,\lvert V_{cs}\rvert^2$
12	$b \to u\, e^-\bar{\nu}\gamma$	$\lvert V_{ub}\rvert^2$
13	$b \to u\, \mu^-\bar{\nu}\gamma$	$\lvert V_{ub}\rvert^2$
14	$b \to u\, \tau^-\bar{\nu}\gamma$	$\lvert V_{ub}\rvert^2$

Table 5: CC radiative b-quark decays contributing to $B \to (X_c, X_u) + \gamma$ and their CKM matrix element dependent factors in decay widths, K_n.

ARGUS and CLEO measurements of the semileptonic branching ratios [6]:

$$\frac{\tau_{B^\pm}}{\tau_{B^0}} = \frac{BR(B^\pm \to D^{(*)0}\ell^\pm\nu)}{BR(B^0 \to D^{(*)-}\ell^+\nu)} = 0.96 \pm 0.14 \qquad (26)$$

as well as from individual B-hadron lifetime measurements from experiments at LEP [40]. We now specify the approximations used in calculating the inclusive photon energy spectrum from the CC processes [15,44]. First, we have left out the QCD corrections to the decays listed in Table 5. Judging from the analogous corrections to the non-radiative b decays, which are typically of $O(20\%)$, we don't expect such corrections to alter the basic description given in [15]. It is to be noted that the radiative semileptonic decays contribute more significantly to the CC radiative B-decays than the purely hadronic ones due to the smallness of the electron and muon mass. Hence, the dominant corrections in CC decays are expected to arise from the leading QCD contribution to the semileptonic radiative decays, including real and virtual gluon bremsstrahlung processes such as $b \to (c,u)\ \ell\nu_\ell + \gamma + g$. These corrections will be needed as the experimental precision on the inclusive photon energy measurements improve. For a first estimate, the CC processes listed in Table 5 are quite adequate. We have also left out the QED virtual corrections in CC decays, as a result of which our calculations are ill-suited for the soft photon energy spectrum in radiative B-decays. There is no overriding experimental interest in the soft photon spectrum either, since it is inundated by the initial state radiation (in e^+e^- production processes) and secondary photons from the pion and kaon decays produced in B-decays and in background processes. Depending on the experimental details, the photon energy spectrum above a certain threshold (say $E_\gamma \geq 1.0\ GeV$ in the B-rest frame) should, however, be reliably given by the sum of the CC contributions in Table 5 and the FCNC contributions discussed in the previous sections. The expressions for the matrix elements of the processes in Table 5 are given in detail in ref. [15]. The photon energy

spectrum from the CC processes is shown in Fig. 5, where the contributions from the decays $B \to X_c\gamma$ and $B \to X_u\gamma$ are given separately.

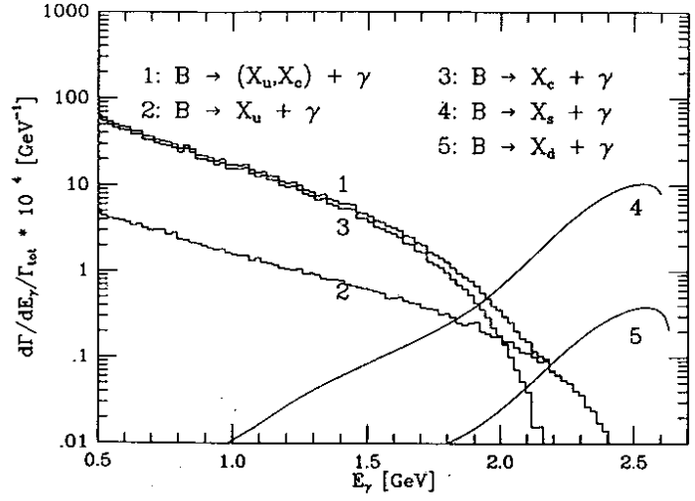

Figure 5: CC and FCNC components of the photon energy spectrum in $B \to X\gamma$

2.3 Inclusive Photon Energy Spectrum in $B \to X + \gamma$

In section 2.1 we have discussed the FCNC contributions to the inclusive photon energy spectrum. Section 2.2 dealt with the CC contributions. We now put together these two components, leading to the inclusive photon energy spectrum in radiative B decays. The results are summarized in Figs. 5 and 6 on which we now want to make a few comments:

- The photon energy spectrum in the decays $B \to X + \gamma$ shown in Fig. 6 divides itself in three regions.

  The first is the low frequency part $E_\gamma \leq 1.8\ GeV$, which is dominated by the CC decay $B \to X_c + \gamma$, a small intermediate region $1.9\ GeV \leq E_\gamma \leq 2.1\ GeV$, where the CC and FCNC contributions are comparable, and the high frequency part $E_\gamma \geq 2.1\ GeV$, which is dominated by the FCNC radiative decay $B \to X_s + \gamma$. Precise measurements of the photon energy spectra in these regions can therefore be used to test the normalization and shape of the two dominating components.

- The significantly different thresholds in the two CC radiative transitions, due to the presence of a charmed hadron in the decays $B \to X_c + \gamma$ versus non-charmed light hadrons in $B \to X_u + \gamma$, result in the longer E_γ-tail for the latter. However, in the region where the photons from the dominant CC process $B \to X_c + \gamma$ range out (say above 2 GeV in the B rest frame), the inclusive photon spectrum is dominated by the CKM allowed FCNC radiative decay $B \to X_s + \gamma$.

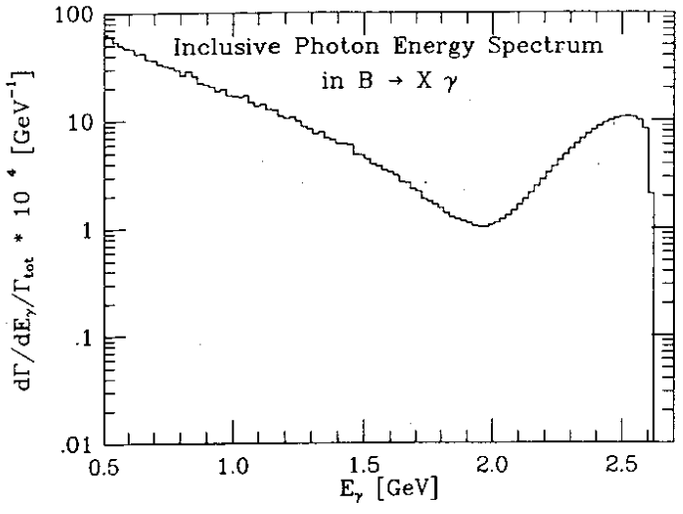

Figure 6: Inclusive photon energy spectrum in $B \to X\gamma$

- The separation of the high frequency part of the spectrum in the two FCNC components $B \to X_s+\gamma$ and $B \to X_d+\gamma$ would require flavour tagging the hadrons recoiling against the photon, for example, by demanding the overall strangeness quantum number of X_d being 0 and of X_s being equal to ± 1. At the exclusive level, this can be exemplified by the decays $B \to K^* + (n\pi) + \gamma$ versus $B \to \rho + (n\pi) + \gamma$.

- Our calculations also indicate that the long distance (i.e. CC) contamination to the short distance piece (i.e. penguin dominated FCNC decays) is small in the high energy region of the photon spectrum. This is a rather important conclusion, since otherwise the final states in the CC radiative decays $B \to X_u+\gamma$ and the FCNC decays $B \to X_d+\gamma$ very easily mock up each other.

- This analysis also demonstrates that probably the most difficult to measure is the CC component $B \to X_u + \gamma$, since there is no region in which it dominates. The only way to isolate this component is probably through the measurement of the photon spectrum in the low frequency part and demanding the absence of charmed hadrons in $B \to X + \gamma$, recoiling against the photon. With a vertex detector, perhaps this is feasible in a limited range of photon energy, though the non-B-background will be formidable, perhaps prohibitive.

3 FCNC B-DECAYS INVOLVING DILEPTONS

In this section, we review the calculations for the FCNC inclusive semileptonic B-decays, $b \to (s,d) + \ell\bar{\ell}$ $(\ell = e,\mu,\tau,\nu)$, and in doing this will treat the quark states synonymous with the corresponding hadron states. Compared to the rare radiative B-decays considered in the previous section, the FCNC semileptonic B-decays $b \to (s,d) + \ell^+\ell^-$ $(\ell = e,\mu,\tau)$ re-

ceive very significant contributions from the so-called long-distance processes. For the dominant decays $b \to s + \ell^+\ell^-$ $(\ell = e,\mu)$, these contributions are dominated by the decays $B \to (J/\psi,\psi')X \to \ell^+\ell^- X$, which have been measured by the ARGUS and CLEO collaborations [18] with a branching ratio $O(10^{-3})$ [18]. However, as the corresponding short distance contribution is estimated to be $O(10^{-6})$ for the decays $b \to s + \ell^+\ell^-$ $(\ell = e,\mu,\tau)$, the long distance contribution in $b \to s + \ell^+\ell^-$ $(\ell = e,\mu)$, while overwhelming near the the J/ψ and ψ' resonances, is still numerically important in the continuum away from the J/ψ and ψ' resonances. Hence, one has to treat the long- and short-distance contributions coherently. We follow here closely the calculations reported in [24], whose sign convention agrees with the choice in [23,46], leading to a constructive interference in the invariant dilepton mass distribution. Inclusive decay rates involving the dielectron and dimuon final states are reported and various distributions sensitive to m_t are shown. At the end of this section we discuss the rates for the FCNC B-decays involving a pair of neutrinos, $b \to (s,d) + \nu\bar{\nu}$. With hermetic detectors and sufficient statistics, this final state may be detected in LEP experiments, or in asymmetric B-factories, if the decay products of the two B-mesons produced in $\Upsilon(4S)$ decays can be separated.

3.1 FCNC B-Decays $B \to (X_s, X_d) + \ell^+\ell^-$

The effective Hamiltonian for the rare decays $b \to (s,d) + \ell\bar{\ell}$ $(\ell = e,\mu,\tau,\nu)$ is derived as before by integrating out the top quark and the W-bosons. We shall concentrate here on the CKM-allowed decays $b \to s + \ell\bar{\ell}$ $(\ell = e,\mu,\tau,\nu)$, but most of what is being said here also applies (with obvious modifications) to the case $b \to d + \ell\bar{\ell}$ $(\ell = e,\mu,\tau,\nu)$. Also, since already the lowest order processes $b \to (s,d) + \ell\bar{\ell}$ $(\ell = e,\mu,\tau,\nu)$ provide a non-trivial lepton-energy and mass-spectra, we shall not consider real gluon bremsstrahlung corrections. This is motivated by the $O(\alpha_s)$ corrections to the rate and spectra in the analogous CC semileptonic decays $b \to (c,u)\ell\nu_\ell$, which lead to at most $O(20\%)$ effects in the decay rates and leave the normalized distributions stable [16,17]. The renormalization group improvements in terms of the Wilson coefficients are, however, included in presenting the rates and distributions being discussed.

In the approximation of keeping only dimension-6 operators, the appropriate basis for the FCNC B-decays involving dileptons consists of twelve operators and the effective Hamiltonian may be written as

$$H_{eff}(b \to s + \ell^+\ell^- \ (\ell = e,\mu,\tau)) = -\frac{4G_F}{\sqrt{2}}\lambda_t \sum_{j=1}^{12} \tilde{C}_j(\mu)\tilde{O}_j(\mu) \qquad (27)$$

Detailed considerations, however, show that the coefficients of some of the operators and their mixing with the remaining ones are small and the basis may be truncated. The operators of interest in the present context are, $\tilde{O}_1, \tilde{O}_2, \tilde{O}_7, \tilde{O}_8$ and $\tilde{O}_9$. The first three in this list were given in the previous section while discussing the decays $b \to s + \gamma + g$. Since the operators $\tilde{O}_j$ are used to calculate the matrix elements for the transition $b \to s$+(virtual) photon, we have to take a one loop matrix element of the operators $\tilde{O}_1, \tilde{O}_2$, and $\tilde{O}_7$. The remaining operators are defined below:

$$\tilde{O}_8 = \frac{\alpha}{4\pi}(\bar{s}\gamma_\mu L b)(\bar{\ell}\gamma_\mu \ell) \qquad (28)$$

$$\tilde{O}_9 = \frac{\alpha}{4\pi}(\bar{s}\gamma_\mu L b)(\bar{\ell}\gamma_\mu\gamma_5 \ell) \qquad (29)$$

and the Wilson coefficients are [11,12]:

$$C_8(m_b) = C_8(M_W) + \frac{4\pi}{\alpha_s(M_W)}\left[\frac{4}{33}\left(1-\eta^{-11/23}\right) - \frac{8}{87}\left(1-\eta^{-29/23}\right)\right] \quad (30)$$

$$C_9(m_b) = C_9(M_W) \quad (31)$$

where we have dropped the tilde on the coefficients $\tilde{C}_i$ for ease of writing. To avoid possible mix-up in the notation, we point out that the operator $\tilde{O}_8$ in the effective Hamiltonian here and the operator $\hat{O}_8$ in the corresponding Hamiltonian for $b \to s + \gamma + g$ are different operators, hence also the Wilson coefficients C_8 in the two cases are different. Again, the large logarithms of the type $\ln(M_W^2/m_b^2)$ are included in the Wilson coefficients and not in the matrix elements of the operators.

The coefficients $C_8(m_W)$ and $C_9(m_W)$ appearing above can be seen in [23,11,12]. The matrix-element for the process of interest can be written as:

$$\mathcal{M}(b \to s + \ell^+\ell^-) = 2\sqrt{2}\, G_F \frac{\alpha}{sin^2\,\theta_W}\lambda_t \frac{-1}{4\pi}\overline{\mathcal{M}} \quad (32)$$

where we have again dropped the small terms due to the intermediate u-quark, and have used the CKM unitarity constraint to relate $\lambda_c \equiv V_{cb}V_{cs}^*$ to λ_t. The reduced matrix element $\overline{\mathcal{M}}$ can be shown to be:

$$\overline{\mathcal{M}} = C_{\mathcal{A}}\,\bar{s}_L\gamma_\mu b_L\,\bar{\ell}_L\gamma^\mu\ell_L + C_{\mathcal{B}}\,\bar{s}_L\gamma_\mu b_L\,\bar{\ell}_R\gamma^\mu\ell_R + 2\sin^2\theta_W C_7(\mu)\bar{s}i\sigma_{\mu\nu}q^\nu/q^2(m_s L + m_b R)b\,\bar{\ell}\gamma_\mu\ell \quad (33)$$

As pointed out earlier, one has to calculate both the long- and short-distance contribution to $\overline{\mathcal{M}}$. We concentrate first on the short distance piece and give the long distance contribution later. The functions $C_{\mathcal{A}}$, $C_{\mathcal{B}}$ are given by:

$$C_{\mathcal{A}} = \sin^2\theta_W(-C_8(m_b) + C_9(m_b) - (3C_1(m_b) + C_2(m_b))g(m_c/m_b, q^2)) \quad (34)$$

$$C_{\mathcal{B}} = \sin^2\theta_W(-C_8(m_b) - C_9(m_b) - (3C_1(m_b) + C_2(m_b))g(m_c/m_b, q^2)) \quad (35)$$

and the function $g(m_c/m_b, q^2)$ arises from the one-loop matrix element of the four-quark operators [23,11]. The invariant dilepton mass distribution in the inclusive decays can now be calculated easily with the help of the matrix elements, given above. For the inclusive decay rate contribution from the short-distance piece, one estimates:

$$BR(B \to X_s + e^+e^-) = (0.6 - 2.5)\times 10^{-5}$$
$$BR(B \to X_s + \mu^+\mu^-) = (3.5 - 14.0)\times 10^{-6} \quad (36)$$

for the top quark mass range 100 GeV $< m_t <$ 200 GeV, whereas for $m_t = 150$ GeV, the central value we are using in this report, one obtains $BR(B \to X_s + e^+e^-) = 1.5\times 10^{-5}$ and $BR(B \to X_s + \mu^+\mu^-) = 8.5\times 10^{-6}$. Thus, FCNC semileptonic decay rates are much more sensitive to m_t than the corresponding FCNC radiative B decays. These estimates are to be contrasted with the recent upper limit for the (averaged) B-meson branching ratio from the UA1 collaboration: $BR(B \to X + \mu^+\mu^-) = 5\times 10^{-5}$ [45], indicating that the present experimental sensitivity is an order of magnitude away in this channel. The branching ratios for the Cabibbo-suppressed FCNC decays $b \to d + \ell^+\ell^-$ ($\ell = e, \mu, \tau$) can be obtained by scaling the corresponding $b \to s + \ell^+\ell^-$ ($\ell = e, \mu, \tau$) rates by the CKM factor $(|V_{td}|/|V_{ts}|)^2$. One expects

$$BR(B \to X_d + \ell^+\ell^-)/BR(B \to X_s + \ell^+\ell^-) = \frac{|V_{td}|^2}{|V_{ts}|^2}(1+\delta) \quad (37)$$

where δ represents the differences due to phase space and SU(3)-breaking effects. The relative rates $BR(B \to X_d + \ell^+\ell^-)/BR(B \to X_s + \ell^+\ell^-)$ are independent of m_t and QCD corrections, and their eventual measurement would determine the indicated CKM matrix-element ratio. The precise value of this ratio depends on the parameters, ρ and η, as discussed in the previous section. However, for the default value, $|V_{td}/V_{cb}| = 0.21$ used in this paper, we estimate a suppression by a factor ~ 22 for the CKM-suppressed FCNC semileptonic decays in SM, yielding (for $m_t = 100 - 200$ GeV):

$$BR(B \to X_d + e^+e^-) = (2.6 - 10.0)\times 10^{-7}$$
$$BR(B \to X_d + \mu^+\mu^-) = (1.5 - 6.0)\times 10^{-7} \quad (38)$$

Some of these decay rates should be measurable at a first generation B-factory and in high energy hadronic collisions, such as at the Tevatron, LHC and SSC.

The calculations so far, however, take into account only the short distance contributions. In addition to this, there are long distance contributions from the intermediate $c\bar{c}$ state. Formally, this contribution can be implemented by the replacement of the function $g(m_c/m_b, q^2)$ by $G(m_c/m_b, q^2)$ in the expressions for $C_{\mathcal{A}}$ and $C_{\mathcal{B}}$ above, where [24],

$$G(m_c/m_b, q^2) = \{g(m_c/m_b, q^2) + \frac{3}{\alpha^2}\kappa \sum_{V_i = \Psi, \Psi'} \frac{\pi\Gamma[V_i \to l^+l^-]M_{V_i}}{M_{V_i}^2 - q^2 - iM_{V_i}\Gamma_{V_i}}\} \quad (39)$$

The pole contributions from the J/ψ and ψ' with the Breit-Wigner form are explicitly indicated.

It is well known that the Wilson coefficient sum $3C_1(m_b) + C_2(m_b)$, entering in the coefficients $C_{\mathcal{A}}$ and $C_{\mathcal{B}}$ in Eqs. (33)-(34) above, depends very sensitively on the QCD scale parameter Λ_{QCD}, as well as the renormalization point μ. For instance, taking $\Lambda_{QCD} = 400$ MeV and the scale $\mu = m_b$ one has $3C_1(m_b) + C_2(m_b) = -0.17$, while for $\Lambda_{QCD} = 100$ MeV one obtains $3C_1(m_b) + C_2(m_b) = -0.41$, and for $\Lambda_{QCD} = 100$ MeV and using the renormalization point $\mu = 2m_b$ one finds $3C_1(2m_b) + C_2(2m_b) = -0.58$. Although the QCD corrected inclusive nonleptonic decay rate is stable against changes in Λ_{QCD}, the semi-inclusive channels $B \to J/\psi X_s$ and $B \to \psi' X_s$ have rather large uncertainties due to cancellations in the relevant combination of the Wilson coefficients.

A good strategy to calculate the inclusive dilepton invariant mass and related distributions in the decays $b \to s + \ell^+\ell^-$ ($\ell = e, \mu, \tau$), pending a satisfactory theoretical resolution of the long-distance puzzle in the decays $B \to (J/\psi, \psi')\, X_s$, is to use the data to calibrate the long-distance contribution. Using the branching ratios from the Particle Data Group [18] $BR(B \to J/\psi X \to l^+l^-X) = BR(B \to J/\psi X)BR(J/\psi \to l^+l^-) \simeq 7\times 10^{-4}$ fixes the constant κ introduced in the resonance part of the amplitude for $b \to s\ell^+\ell^-$. Numerically, a value $\kappa(3C_1(m_b) + C_2(m_b)) = -1$ reproduces the data well. Curiously, this amounts to neglecting the QCD corrections in the decay $B \to (J/\psi, \psi')X_s$, since $3C_1(m_W) + C_2(m_W) = -1$.

Fixing the normalization of the long distance piece from data, we show two differential distributions here, namely the dilepton invariant mass and the forward-backward asymmetry of the charged lepton l^+ in the rest frame of the dilepton pair. Defining the variable $z \equiv \cos\theta$, as the angle between the momentum of the B-meson and that of lepton l^+ in the rest frame of the dilepton, the forward-backward asymmetry for a fixed invariant mass q^2 is obtained by integrating the double differential branching ratio $(\frac{d^2BR}{dq^2dz})$ with respect to the angular variable

z,

$$A(q^2) \equiv \frac{\int_0^1 dz \frac{d^2BR}{dq^2 dz} - \int_{-1}^0 dz \frac{d^2BR}{dq^2 dz}}{\int_0^1 dz \frac{d^2BR}{dq^2 dz} + \int_{-1}^0 dz \frac{d^2BR}{dq^2 dz}} \tag{40}$$

In the region where $A(q^2)$ is positive, the number of l^+ scattered in the forward hemisphere is more than the one in the backward hemisphere in the center of mass frame of the dilepton.

The asymmetry in the dilepton angular distribution can be qualitatively understood as follows. The decays $b \to s + \ell^+\ell^-$ ($\ell = e, \mu, \tau$) occur through γ , Z and W^+W^- exchange diagrams. For low m_t ($\frac{m_t}{M_W} < 1$) the photon contribution dominates and the vector-like interactions to the leptonic current remain substantial, consequently the asymmetry is small. However, for $\frac{m_t}{M_W} > 1$, the contribution from the Z-exchange diagrams becomes important and the coefficient of the left-handed leptonic current grows as m_t^2, leading to a large asymmetry. (A part of the coefficient for the vector current also behaves in the same way because Z also couples to the vector current.) It should be noted that the asymmetry depends on the invariant dilepton mass. At and near the J/ψ and ψ' peaks, the asymmetry is small since the resonances couple to the vector leptonic current.

3.2 Dilepton Invariant-mass and Asymmetry Distributions in $B \to (X_s, X_d) + \ell^+\ell^-$

Some results of interest taken from [24] are summarized in Figs. 7 and 8. In Fig. 7, we show the invariant dilepton mass distribution, $dBR/d\hat{s}$, for three assumed values of the top quark mass, $m_t = 100,\ 150,\ 200\ GeV$. Here, the variable $\hat{s}$ is the normalized dilepton invariant-mass, $\hat{s} = m_{\ell\ell}^2/m_b^2$. Away from the resonance regions, $m_{\ell\ell}^2 = m_{J/\psi,\psi'}^2$, the dilepton mass distribution is sensitive to the top quark mass. This can also be seen quantitatively in Table 6, where the branching ratios, integrated over well defined regions of the dilepton invariant mass in the decays $B \to X_s + \ell^+\ell^-$, with $\ell = e, \mu$, are shown. To test the dynamics of the short distance component (and hence to gain sensitivity on m_t), it will be crucial to measure the dilepton mass spectra in the regions called (i), (iii), and (v) in Table 6. We recall here that the present experimental limit on $b \to s + \ell^+\ell^-$ ($\ell = e, \mu, \tau$) is based on the analysis of the region (v) by the UA1 collaboration. The double differential distribution evaluated at

$m_t(GeV)$	(i)	(ii)	(iii)	(iv)	(v)
100	1.8×10^{-6}	6.8×10^{-4}	4.3×10^{-7}	3.3×10^{-5}	1.8×10^{-7}
150	2.7×10^{-6}	6.8×10^{-4}	6.6×10^{-7}	3.3×10^{-5}	4.1×10^{-7}
200	4.3×10^{-6}	6.8×10^{-4}	1.1×10^{-6}	3.3×10^{-5}	8.5×10^{-7}

Table 6: Branching ratio for the decay $B \to X_s + \ell^+\ell^-$ with $\ell = e, \mu$ in different regions of the dilepton invariant mass, $s = m_{\ell\ell}^2$. (i): 1.0 GeV$^2 \le s \le (M_{J/\psi} - \delta)^2$, (ii): $(M_{J/\psi} - \delta)^2 \le s \le (M_{J/\psi} + \delta)^2$, (iii): $(M_{J/\psi} + \delta)^2 \le s \le (M_{\psi'} - \delta)^2$, (iv): $(M_{\psi'} - \delta)^2 \le s \le (M_{\psi'} + \delta)^2$, (v): $(M_{\psi'} + \delta)^2 \le s \le (M_b - M_s)^2$, where an energy resolution of $\delta = 20$ MeV at the J/ψ and ψ' resonances has been assumed (from ref. [24]).

the point $\hat{s} = 0.3$, $d^2BR/d\hat{s}dz|_{\hat{s}=0.3}$ is shown in Fig. 8 for $m_t = 100,\ 150,\ 200$ GeV. The asymmetry for the decays $b \to s + \ell^+\ell^-$ ($\ell = e, \mu, \tau$), defined above, in three different invariant

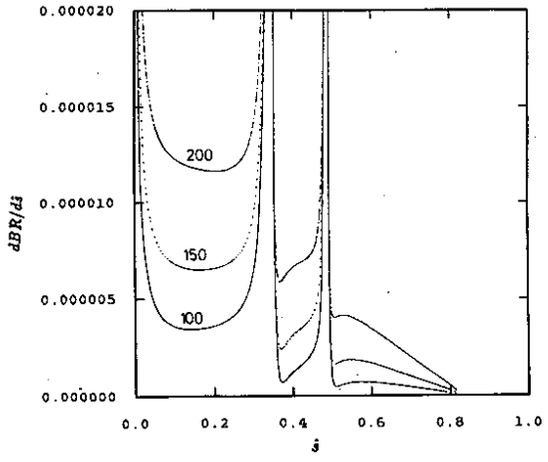

Figure 7: The differential branching ratio $dBR/d\hat{s}$ as a function of the scaled invariant dilepton mass $\hat{s} = s/m_b^2$ in the decay $b \to s + \ell^+\ell^-$ ($\ell = e, \mu, \tau$). Assumed top quark mass values are indicated on the curves (from ref. [24]).

dilepton mass ranges for the assumed values of the top quark mass, $m_t = 100,\ 150,\ 200$ GeV, can be seen in ref. [24].

3.3 Estimates of the FCNC B-Decays $B \to (X_s, X_d) + \nu\bar{\nu}$

As the final inclusive rare B-decays, we take up the FCNC B-decays involving two neutrinos $b \to (s, d) + \nu\bar{\nu}$. The exclusive decays in this chain, involving for example $B \to (K, \pi)\nu\bar{\nu}$ and $B \to (K^*, \rho)\nu\bar{\nu}$, will be discussed in the next section. The FCNC dineutrino B-decays are experimentally very difficult to measure, except probably in a high luminosity LEP environment, involving the decay $Z^0 \to b\bar{b}$, where such events have a nice tag: large missing energy and momentum in a b-quark jet with no charged lepton. From the theoretical point of view, on the other hand, these decays are much simpler to deal with, since the operator basis given for $b \to s + \ell\bar{\ell}$ ($\ell = e, \mu, \tau, \nu$) reduces to only one operator, which is the difference of the $\tilde{O}_8$ and $\tilde{O}_9$ operators. Thus, a left handed current for the neutrino appears which couples pointlike to the left handed current of the $b \to s$ transition. The Wilson coefficient of this operator is D_9 [47]

$$D_9(M_W) = \frac{1}{\sin^2\theta_W}\left[\frac{1}{8}x + \frac{3}{8}\frac{x(x-2)}{(x-1)^2}\ln x + \frac{3}{8}\frac{x}{x-1}\right] \tag{41}$$

D_9, like C_9, is not affected by the QCD scaling corrections. This gives

$$H_{eff}(b \to s + \nu\bar{\nu}) = -\frac{8G_F}{\sqrt{2}}V_{tb}V_{ts}^* D_9(M_W)\left(\frac{\alpha}{4\pi}\right)(\bar{s}\gamma_\mu L b)(\bar{\nu}\gamma_\mu L\nu) \tag{42}$$

The differential distribution in the missing invariant mass for the inclusive decay $b \to s + \nu\bar{\nu}$ are given in [25], together with the corresponding distributions for some exclusive decays. The

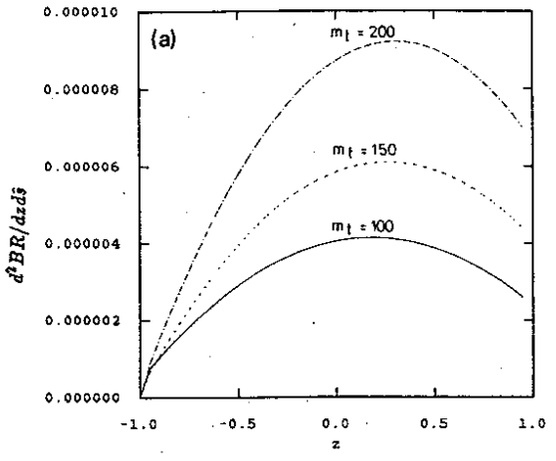

Figure 8: The angular distribution $d^2BR/d\hat{s}dz|_{\hat{s}=0.3}$ in the decay $b \to s + \ell^+\ell^-$ ($\ell = e, \mu, \tau$) as a function of the variable z for the indicated values of the top quark mass (from ref. [24]).

branching ratios for the inclusive decays $B \to X_s + \nu\bar{\nu}$, summed over three neutrino species, and $m_t = 100 - 200$ GeV, has been estimated as [25]:

$$BR(B \to X_s + \nu\bar{\nu}) = (2.8 - 13.0) \times 10^{-5} \tag{43}$$

with $BR(B \to X_s + \nu\bar{\nu}) = 6.8 \times 10^{-5}$ for $m_t = 150$ GeV. These decays, like their charged dilepton counterparts, are sensitive to m_t. Again, for the CKM-suppressed inclusive decays $BR(B \to X_d + \nu\bar{\nu})$, one expects:

$$\frac{BR(B \to X_d + \nu\bar{\nu})}{BR(B \to X_s + \nu\bar{\nu})} = \frac{|V_{td}|^2}{|V_{ts}|^2}. \tag{44}$$

For the default value of $|V_{td}/V_{cb}| = 0.21$ used in this paper, this gives giving

$$BR(B \to X_d + \nu\bar{\nu}) = (1.2 - 5.6) \times 10^{-6} \tag{45}$$

Again, prototypes of this class would be $B \to (\pi, \rho)\, \nu\bar{\nu}$, which can be related to the corresponding CC decays.

4 Exclusive Rare B Decays

In this section we shall discuss exclusive rare B decays. These fall into three classes. The first class consists of the purely leptonic decays like $B_d^0 \to \ell^+\ell^-$ and $B_s^0 \to \ell^+\ell^-$ where $\ell = e, \mu, \tau$. In SM the decays $B_d^0 \to \ell^+\ell^-$ will be suppressed due to their dependence on the CKM matrix element $|V_{td}|$ and helicity, leading to a factor m_l^2/m_B^2 in rates. Consequently, the branching fractions are very small, see table (14), thus such decays will be too small to be observable even in a first generation B factory. However, one has to keep in mind that the small branching fractions for the purely leptonic modes are SM predictions and thus an

observation of such processes would be a sign of physics beyond the Standard Model. In particular, leptoquarks in the TeV mass range can induce measurable rates for the decays such as $(B_d, B_s) \to \ell^+\ell^-$ [48].

The second class of exclusive B decays that we want to discuss consists of the radiative rare decays. We shall discuss in the next section in some detail the decays $B \to (K^*, K^{**}) + \gamma$ where K^{**} denotes any excited K meson, some of which are listed in Table 7.

The third class of exclusive decays that we discuss are the semileptonic FCNC decays. We shall consider in some detail the decays involving charged leptons like $B \to K^{(*)}\, \ell^+\ell^-$ as well as the decays into neutrino pairs like $B \to K^{(*)}\, \nu\bar{\nu}$. Likewise, the FCNC transition $b \to d$, giving rise to the decays $B \to (\pi, \rho)\, \ell^+\ell^-$ as well as $B \to (\pi, \rho)\, \nu\bar{\nu}$, are modes of great theoretical interests, and we also take up their rate estimates here.

4.1 Exclusive radiative rare decays

In this section we shall consider the radiative rare decays into K^* and excited states. In order to arrive at quantitative predictions some input is necessary to model the form factors of the corresponding transition matrix elements. In the following we shall use the relations between the form factors implied by heavy quark symmetries. Although the s quark is not particularly heavy and very substantial corrections to the Isgur-Wise functions are to be anticipated, yet we feel that the heavy quark symmetry can be used gainfully to relate various form factors.

Heavy quark spin symmetry predicts that heavy hadrons fall into spin symmetry doublets [20]. The corresponding group theory, including excited states, has been elaborated in [49]. The main result is that for transitions from a heavy 0^- ground state meson to a heavy excited meson only one independent form factor per spin symmetry doublet appears. We shall use the model by Grinstein, Scora, Isgur and Wise [50] to estimate the various Isgur-Wise functions.

A rich spectrum of states has been observed in the K system. In Table 7 we summarize the present knowledge about the K, K^* mesons and excited states [18]. In dedicated B-physics experiments, radiative B-decays can be used to check and in some ambiguous cases determine the spin-parity assignment of the various excited states. We use the usual notation for the quantum numbers. The radial excitation quantum number is denoted by $n = 1, 2, 3, \cdots$. $L = (S = 0), (P = 1), (D = 2), \cdots$ is the orbital angular momentum, $s = 0, 1$ is the sum of the spins of the two quarks in the meson and finally $J = 1, 2, 3, \cdots$ is the total spin of the meson. The parity is given by the orbital angular momentum to be $P = (-1)^{L+1}$.

The K resonances listed in Table 7 have to be assigned to spin symmetry doublets. In total we shall consider five spins symmetry doublets

$$(C, C^*) \quad \ell = 0, \quad j_{light} = 1/2 \quad J^P = (0^-, 1^-) \tag{46}$$
$$(E, E^*) \quad \ell = 1, \quad j_{light} = 1/2 \quad J^P = (0^+, 1^+) \tag{47}$$
$$(F, F^*) \quad \ell = 1, \quad j_{light} = 3/2 \quad J^P = (1^+, 2^+) \tag{48}$$
$$(G, G^*) \quad \ell = 2, \quad j_{light} = 3/2 \quad J^P = (1^-, 2^-) \tag{49}$$
$$(C_2, C_2^*) \quad \ell = 0, \quad j_{light} = 1/2 \quad J^P = (0^-, 1^-) \tag{50}$$

We have also included the spins symmetry doublet (C_2, C_2^*) which we consider to be a radial excitation of the lowest spin symmetry doublet. The single independent form factor per spins symmetry doublet is labelled by a corresponding subscript

$$\xi_C(vv') \qquad \text{for} \quad 0^- \to (0^-, 1^-) = (C, C^*) \tag{51}$$

Name	State	J^P	$n^{2s+1}L_J$	$[j_{light}]$	Mass/MeV
K	C	0^-	1^1S_0	$[1/2]$	497.67± 0.03
$K^*(892)$	C^*	1^-	1^3S_1	$[1/2]$	896.1 ± 0.3
$K_1(1270)$	E^*	1^+	$1^1P_1/1^3P_1$	$[1/2]$	1270 ±10
$K_1(1400)$	F	1^+	$1^1P_1/1^3P_1$	$[3/2]$	1402 ± 7
$K^*(1410)$	C_2^*	1^-	2^3S_1	$[1/2]$	1412 ±12
$K^*(1430)$	E	0^+	1^3P_0	$[1/2]$	1429 ± 7
$K_2^*(1430)$	F^*	2^+	1^3P_2	$[3/2]$	1425.4 ± 1.3
$K(1460)$	C_2	0^-	2^1S_0	$[1/2]$	≈1460
$K_2(1580)$	G^*	2^-	$[1^1D_2/1^3D_2]$	$[3/2]$	≈1580
$K_1(1650)$		1^+	$[2^1P_1]$	$[1/2]$	1650 ±50
$K^*(1680)$	G	1^-	1^3D_1	$[3/2]$	1714 ±20
$K_2(1770)$		2^-	$[1^1D_2/]1^3D_2$	$[5/2]$	1768 ±14
$K_3^*(1780)$		3^-	1^3D_3	$[5/2]$	1770 ±10
$K(1830)$		0^-	3^1S_0	$[1/2]$	≈1830
$K_0^*(1950)$		0^+	$[2^3P_0]$	$[1/2]$	1945 ±32
$K_2^*(1980)$		2^+			1975 ±22
$K_4^*(2045)$		4^+	1^3F_4		2045 ± 9
$K_2(2250)$		2^-			2247 ±17
$K_3(2320)$		$3+$			2324 ±24
$K_5^*(2380)$		5^-			2382 ±24
$K_4(2500)$		4^-			2490 ±20

Table 7: Spectrum of neutral K mesons. Notation, masses, and assignment of quantum numbers are taken from [18], except for quantities in brackets. The systematical and statistical errors on the masses have been added in quadrature.

$$\xi_{C_2}(vv') \quad \text{for} \quad 0^- \to (0^-, 1^-) = (C_2, C_2^*) \tag{52}$$
$$\xi_E(vv') \quad \text{for} \quad 0^- \to (0^+, 1^+) = (E, E^*) \tag{53}$$
$$\xi_F(vv') \quad \text{for} \quad 0^- \to (1^+, 2^+) = (F, F^*) \tag{54}$$
$$\xi_G(vv') \quad \text{for} \quad 0^- \to (1^-, 2^-) = (G, G^*) \tag{55}$$

where v and v' denote the velocities of the incoming and outgoing meson, respectively. The assignment of the resonances to spin symmetry doublets is not unique. We shall choose our assignment of the excited K mesons into the spin symmetry doublets in the following way: we put the $K_1(1270)$ and the $K_2^*(1430)$ into the spin symmetry doublet (E, E^*) and correspondingly the $K_1(1400)$ and the $K(1430)$ into (F, F^*). In particular, this assignment of the states $K_1(1270)$ and $K_1(1400)$ implies that due to the spin symmetry these states will be a mixture of the quark model states 1^1P_1 and 1^3P_1 with a mixing angle of 45°. In fact, this value of the mixing angle is consistent with experimental results [51], which in turn supports our assignment of the states to the spin symmetry doublets. A further motivation for our assignment is the fact that in the D system the lowest lying 1^+ state is the spin symmetry partner of the lowest 2^+ state. We shall put the $K^*(1680)$ and the $K_2(1580)$ into a fourth spin symmetry doublet (G, G^*), assuming that they have both orbital angular momentum $L = 2$. Finally we assume that the $K^*(1460)$ and $K^*(1410)$ are radially excited states, which form a fifth spin symmetry doublet $(C, C^*)_2$.

The effective Hamiltonian for the radiative decays is given in Eq. (5), where only the operator $\mathcal{O}_7$ has a nonvanishing matrix element in the case of radiative decays. Calculating the matrix elements of $\mathcal{O}_7$ for heavy s quark using the representations from [49] for the excited states one finds for the rates in terms of the Isgur-Wise functions (51-55) [2]

$$\Gamma(B \to K^*\gamma) = \Omega\,|\xi_C(vv')|^2\,\frac{1}{y}\left[(1-y)^3(1+y)^5(1+y^2)\right] \tag{56}$$
$$\Gamma(B \to K_1(1270)\gamma) = \Omega\,|\xi_E(vv')|^2\,\frac{1}{y}\left[(1-y)^5(1+y)^3(1+y^2)\right] \tag{57}$$
$$\Gamma(B \to K_1(1400)\gamma) = \Omega\,|\xi_F(vv')|^2\,\frac{1}{24y^3}\left[(1-y)^5(1+y)^7(1+y^2)\right] \tag{58}$$
$$\Gamma(B \to K_2^*(1430)\gamma) = \Omega\,|\xi_F(vv')|^2\,\frac{1}{8y^3}\left[(1-y)^5(1+y)^7(1+y^2)\right] \tag{59}$$
$$\Gamma(B \to K^*(1680)\gamma) = \Omega\,|\xi_G(vv')|^2\,\frac{1}{24y^3}\left[(1-y)^7(1+y)^5(1+y^2)\right] \tag{60}$$
$$\Gamma(B \to K_2(1580)\gamma) = \Omega\,|\xi_G(vv')|^2\,\frac{1}{8y^3}\left[(1-y)^7(1+y)^5(1+y^2)\right] \tag{61}$$
$$\Gamma(B \to K^*(1410)\gamma) = \Omega\,|\xi_{C_2}(vv')|^2\,\frac{1}{y}\left[(1-y)^3(1+y)^5(1+y^2)\right] \tag{62}$$

The argument vv' of the Isgur-Wise functions is fixed by the condition

$$vv' = \frac{m_B^2 + m_{K^{**}}^2}{2m_B m_{K^{**}}} \tag{63}$$

[2] Note that in ref. [26], a factor $(1-y)^2$ was missing in all the expressions listed here, which we now correct. The branching ratios presented in ref. [26] remain unchanged. We thank M. Gourdin and N. Paver for pointing out this typographical error.

and we have used the following abbreviations

$$\Omega = \frac{\alpha}{128\pi^4} G_F^2 m_b^5 |V_{tb}|^2 |V_{ts}|^2 |C_7(m_b)|^2, \quad y = \frac{m_{K^{**}}}{m_B}. \tag{64}$$

Since the decays into states in the same spin symmetry doublet are described by a single Isgur-Wise function, spin symmetry relates these decays. From (56-62) we find

$$\begin{aligned} \Gamma(B \to K_2^*(1430)\gamma) &= 3 \cdot \Gamma(B \to K_1(1400)\gamma) \\ \Gamma(B \to K_2(1580)\gamma) &= 3 \cdot \Gamma(B \to K^*(1680)\gamma) \end{aligned} \tag{65}$$

In the heavy quark limit the two members of a spin symmetry doublet should be degenerate in mass, which means that the corresponding Isgur Wise functions would be taken at the same value of vv' and the ratio y would be the same for both states. However, for the s quark we expect a large breaking of the spin symmetry, which means that the two relations (65) will be only approximate.

In order to obtain quantitative results a model has to be used to actually calculate the Isgur-Wise functions. We shall employ the model by Grinstein, Scora, Isgur and Wise [50]. They use harmonic oscillator wave functions for the mesons. The corresponding oscillator strengths are β_K and β_B which have been fitted in [50] to semileptonic B and D decays. From this fit one obtains $\beta_K = 0.34$ GeV, $\beta_B = 0.41$ GeV, which are not equal and hence the GISW wave functions don't have a built-in flavour symmetry. The breaking of the heavy flavour symmetry causes a violation of the normalization condition $\xi_C(1) = 1$. To estimate the model dependence and the effect of the breaking of heavy quark symmetry we use the same parameter β for both wave functions and vary it between β_K and β_B, hoping that this provides a plausible range for the decay rate predictions.

Table 8 shows our estimates for the exclusive $B \to K^{**}\gamma$ branching ratios. Our results are given in units of the inclusive branching ratio $B \to X_s\gamma$, which has been discussed in section 2. We recall that we estimated an inclusive branching ratio of $BR(B \to X_s\gamma) = 2 - 5 \times 10^{-4}$. For the numerical values of the $B \to K^{**}\gamma$ branching ratios in $BR(B \to X_s\gamma) = 4 \times 10^{-4}$, corresponding to a top quark mass of about 150 GeV and $\mu = m_b$.

For an earlier calculation of $BR(B \to K^*\gamma)$, see ref. [52]. Our predictions for this mode encompasses the estimate $R = 7\%$ from this work. To compare the numbers in Table 8 with the results of the calculation reported in [53], we note first that the experimental information on the K^{**} resonances has increased considerably. Taking into account updated mass values, our results are generally in agreement with [53]. However, there is a noticeable difference in our prediction for the branching fraction into $K_2^*(1430)$, which from our estimate is about a factor three larger compared to the one reported in [53]. Very recently, some of the branching ratios estimated by us in Table 8 have also been calculated in ref. [54] in SM and in the extension of SM with additional charged Higgs doublet. These authors find that the decay mode $B \to K^*(1410)\,\gamma$ is the dominant decay channel in $B \to X_s\,\gamma$. Our result is consistent with spin symmetry, because it satisfies the general relations (65) which hold without model dependent input for the Isgur-Wise functions. However, one should anticipate significant power corrections, which have yet to be estimated. It is obvious that a B factory will be able to thoroughly scan the K^{**}-mass region, via FCNC B decays, and it should be possible to distinguish various competing models. Our aim at this stage is to get ball-park estimates. Obviously, there is much room here for theoretical improvements.

Name	State	J^P	vv'	ξ	R	$BR \times 10^{-5}$
K	C	0^-	5.346	0.125 – 0.239	forbidden	forbidden
K^*	C^*	1^-	3.030	0.136 – 0.253	3.5% – 12.2%	1.4 – 4.9
$K^*(1430)$	E	0^+	1.982	0.309 – 0.453	forbidden	forbidden
$K_1(1270)$	E^*	1^+	2.198	0.296 – 0.441	4.5% – 10.1%	1.8 – 4.0
$K_1(1400)$	F	1^+	2.015	0.307 – 0.451	6.0% – 13.0%	2.4 – 5.2
$K_2^*(1430)$	F^*	2^+	1.987	0.309 – 0.452	17.3% – 37.1%	6.9 – 14.8
$K^*(1680)$	G	1^-	1.702	0.359 – 0.420	1.1% – 1.5%	0.4 – 0.6
$K_2(1580)$	G^*	2^-	1.820	0.350 – 0.417	4.5% – 6.4%	1.8 – 2.6
$K(1460)$	C_2	0^-	1.946	-0.242 – -0.293	forbidden	forbidden
$K^*(1410)$	C_2^*	1^-	2.005	-0.240 – -0.292	7.2% – 10.6%	2.9 – 4.2
Sum					44.1% – 90.9%	17.6 – 36.4

Table 8: Values for the Isgur-Wise function, the exclusive to inclusive ratio $R = \Gamma(B \to K^*\gamma)/\Gamma(B \to X_s\gamma)$, and the branching ratio $BR(B \to K^*\gamma)$ for K^* and higher resonances, taken from ref. [26].

4.2 Semileptonic Rare B Decays

In this section we shall consider in some detail the semileptonic rare decays $B \to K^{(*)}\ell^+\ell^-$. In this case all the operators $\mathcal{O}_1$ to $\mathcal{O}_9$ of the operator basis for the effective Hamiltonian (Eq. (5)) contribute. We shall take two complementary points of view. One may exploit heavy quark symmetries of heavy to light transitions to obtain a relation between semileptonic heavy to light decays and the rare decays. However, this approach only allows to relate these decays and will not yield absolute predictions. In order to arrive at absolute predictions we shall again use the relations between form factors obtained in the limit of heavy s quark. We shall use two parametrizations of the Isgur-Wise function, fitted to the semileptonic D-decays.

First, we apply heavy quark symmetries and treat the s quark as a light quark, i.e. we have to consider a heavy to light decay. This has been done first in [55] where the relations we are going to exploit have been derived first. The main idea is that the spin flavour symmetries of the heavy quark limit may be used to relate heavy to light decays, in particular the semileptonic ones with the rare decays. Thus one finds relations among the rare decay $B \to K\ell^+\ell^-$ and the semileptonic decays $B \to \pi\ell\,\nu_\ell$, $D \to \pi\ell\nu_\ell$ and $D \to K\,\ell\nu_\ell$. By the same token, one may relate $B \to K^*\ell^+\ell^-$ to the semileptonic decays $B \to \rho\,\ell\nu_\ell$, $D \to \rho\ell\nu_\ell$ and $D \to K^*\,\ell\nu_\ell$. In addition, heavy quark symmetries also allow to relate the rare decays $B \to K^{(*)}\,\nu\bar{\nu}$ to the corresponding semileptonic decays.

Heavy quark symmetries will work best in the region close to the maximal momentum transfer to the leptons and we shall restrict ourselves to the comparison of the lepton spectra of the processes mentioned above close to the point of maximal momentum transfer. Experimentally this will be the kinematic region where most of the data will be obtained and a comparison of the spectra should be within reach of a future B factory.

In addition to heavy flavour symmetry one needs also the usual flavour $SU(3)$ symmetry. However, flavour $SU(3)$ is broken by the hadron masses and in form factors. The kinematic effects of $SU(3)$ breaking may easily be taken into account by using the measured value for

$m_K/m_\pi \sim 3.7$. We shall assume in the following that $SU(3)$ breaking in the form factors is negligible.

For the decays into a light pseudoscalar meson, close to the point of maximal momentum transfer to the leptons, one has for the ratio of the spectra of $B \to K\ell^+\ell^-$ and $B \to \pi\, e\nu$ [27]:

$$\begin{aligned}\tilde{R}_\ell(z) &\equiv \frac{\frac{d\Gamma}{dz}(B \to K\ell^+\ell^-)}{\frac{d\Gamma}{dz}(B \to \pi\, e\nu)} \\ &= \frac{|V_{ts}V_{tb}^*|^2}{|V_{ub}|^2}\frac{\alpha^2}{8\pi^2}\left(\frac{z^2-4\kappa^2}{z^2-4r^2}\right)^{3/2}\left\{|C_{8eff}+2C_7|^2+|C_9|^2\right\}\end{aligned} \tag{66}$$

where $z = (2v\cdot p)/m_B$, $r = m_\pi/m_B$, and $\kappa = m_K/m_B$; v and p are the velocity of the decaying B meson and the momentum of the final state light meson, respectively. Note that in the limit $\kappa \to r$ this ratio depends only weakly on z through the coefficient C_{8eff}, calculated from the quark loop diagrams. Inserting the maximum value for the momentum transfer the ratio $\tilde{R}_\ell$ becomes a constant in the limit $\kappa = r$,

$$\tilde{R}_\ell = \frac{|V_{ts}V_{tb}^*|^2}{|V_{ub}|^2}\frac{\alpha^2}{8\pi^2}\left\{|C_{8eff}+2C_7|^2+|C_9|^2\right\} \tag{67}$$

This relation is model independent and relates the lepton spectra of the usual, i.e. CC -induced, and the rare, i.e., FCNC-induced, semileptonic decays; it will be of some use at a future B factory since both the decays $B \to K\ell^+\ell^-$ and $B \to \pi\, e\nu$ will hopefully be measured.

Similarly, one may also relate the rare FCNC B-decays to the semileptonic D decay $D \to K\, e\nu$, obtaining

$$\frac{\frac{d\Gamma}{d(v\cdot p)}(B \to K\ell^+\ell^-)}{\frac{d\Gamma}{d(v\cdot p)}(D \to K\, e\nu)} = \frac{m_B^2}{m_D^2}\tilde{R}_\ell \tag{68}$$

The decays into light vector mesons may be treated in an analogous way. One may compare the semileptonic decays $B \to \rho\, e\nu$ and $D \to K^*\, e\nu$ with the short distance piece of $B \to K^*\ell^+\ell^-$. The flavour $SU(3)$ mass splitting for the vector mesons is much smaller than for the pseudoscalars and we may neglect the kinematic factors originating from the different masses of the light mesons. The ratio between the decays $B \to \rho\, e\nu$ and $B \to K^*\, \ell^+\ell^-$ is given by

$$\frac{\frac{d\Gamma}{dz}(B \to K^*\ell^+\ell^-)}{\frac{d\Gamma}{dz}(B \to \rho\, e\nu)} = \tilde{R}_\ell \tag{69}$$

and thus this ratio is equal to the ones appearing in the decays into light pseudoscalar mesons.

We can also relate the rare decay to the semileptonic decay $D \to K^* e\nu$ which for small energies results in the same constant ratio as in the pseudoscalar case

$$\frac{\frac{d\Gamma}{d(v\cdot p)}(B \to K^*\ell^+\ell^-)}{\frac{d\Gamma}{d(v\cdot p)}(D \to K^*\, e\nu)} = \frac{m_B^2}{m_D^2}\tilde{R}_\ell \tag{70}$$

The Wilson coefficients depend on m_t which translates into the m_t-dependence of $\tilde{R}_\ell$. We list in Table (9) the values of $\tilde{R}_\ell$ for different top masses in units of the value at $m_t = 100$ GeV

$$R_\ell(m_t = 100\ GeV) = \frac{|V_{ts}V_{tb}^*|^2}{|V_{ub}|^2}\cdot(7.42\times10^{-6}) \simeq 1.16\times10^{-3} \tag{71}$$

where we have used the default values for the CKM matrix elements from Table 1.

Finally, we discuss the rates for the FCNC semileptonic decays $B \to (K, K^*)\, \nu\bar{\nu}$. In the same way as for the decays into charged leptons one finds for the rare decays into neutrinos a constant ratio depending on the Wilson coefficient D_9 appearing in the effective Hamiltonian for the decays into neutrino pairs. One finds

$$\begin{aligned}R_\nu &\equiv \frac{\frac{d\Gamma}{d(v\cdot p)}(B \to K\ \nu\bar{\nu})}{\frac{d\Gamma}{d(v\cdot p)}(D \to K\ e\nu)} \\ &= \left|\frac{V_{ts}V_{tb}^*}{V_{cs}}\right|^2\frac{m_B^2}{m_D^2}\frac{\alpha^2}{8\pi^2}\,6|D_9|^2 = \left|\frac{V_{ts}V_{tb}^*}{V_{cs}}\right|^2\cdot 4.55\cdot10^{-4} = 9.3\cdot10^{-7}\end{aligned} \tag{72}$$

where a top mass of 100 GeV, $|V_{ts}| = 0.044$ and $|V_{cs}| = 0.974$ have been used. The dependence on m_t of the ratio R_ν is displayed in Table 10.

m_t [GeV]	100	125	150	175	200	225	250
$\tilde{R}_\ell(m_t)/\tilde{R}_\ell(100\ \text{GeV})$	1.0	1.5	2.1	2.9	4.0	5.4	7.1

Table 9: Top mass dependence of the ratio $\tilde{R}_\ell$

m_t [GeV]	100	125	150	175	200	225	250
$R_\nu(m_t)/R_\nu(100\ \text{GeV})$	1.0	1.6	2.4	3.4	4.7	6.2	8.0

Table 10: Top mass dependence of the ratio R_ν

The spectra of the lepton invariant mass may be expressed in terms of the Isgur-Wise function and the corresponding expressions may be found in [25]. In order to obtain the decay rates we have to specify a parametrization of the Isgur-Wise function. We shall use two different parametrizations; the first one is inspired by a monopole form:

$$\xi(v\cdot v') = \frac{w_0^2}{w_0^2 - 2 + 2v\cdot v'} \tag{73}$$

and the second one by models employing wave functions to calculate the decay form factors:

$$\xi(v\cdot v') = \exp\left(\beta(1 - v\cdot v')\right) \tag{74}$$

We use the total rates of the decay $D \to K\ \ell\nu_\ell$ to fit w_0 in (73) and β in (74). The best fit is obtained for $w_0 \approx 1.80$ and $\beta \approx 0.5$ [25]. These two parametrizations may be used to integrate the differential rates as given in [25] and the numerical results are displayed in Table 11 for the decay $B \to K\ell^+\ell^-$ and in Table 12 for the decay $B \to K^*\ell^+\ell^-$. Note that the differential rate for $B \to K^*e^+e^-$ behaves like $1/m_\ell^2$ for small invariant dilepton masses m_ℓ^2 and thus the total rate will depend logarithmically on the lower bound of the integration, namely $4m_\ell^2/m_B^2$. This is the only point in our analysis where lepton mass effects become important. The rate $B \to Kee$ does not become singular in this limit, and thus the difference

	Eq. (73), $w_0 = 1.80$	Eq. (74), $\beta = 0.50$
$\Gamma(B \to K\ell^+\ell^-)$ /GeV	$2.9 \cdot 10^{-19}$	$1.3 \cdot 10^{-19}$
$BR(B \to K\ell^+\ell^-)$	$6.0 \cdot 10^{-7}$	$2.7 \cdot 10^{-7}$
$R(B \to Ke^+e^-)$	4%	2%
$R(B \to K\mu^+\mu^-)$	7%	3%

Table 11: Rates and branching fractions for the decays $B \to K\ell^+\ell^-$ with $\ell = e, \mu$, and $m_t = 150$ GeV.

	Eq. (73), $w_0 = 1.80$	Eq. (74), $\beta = 0.50$
$\Gamma(B \to K^*e^+e^-)$ /GeV	$2.7 \cdot 10^{-18}$	$2.0 \cdot 10^{-18}$
$BR(B \to K^*e^+e^-)$	$5.6 \cdot 10^{-6}$	$4.1 \cdot 10^{-6}$
$R(B \to K^*e^+e^-)$	37%	28%
$\Gamma(B \to K^*\mu^+\mu^-)$ /GeV	$1.4 \cdot 10^{-18}$	$1.2 \cdot 10^{-18}$
$BR(B \to K^*\mu^+\mu^-)$	$2.9 \cdot 10^{-6}$	$2.5 \cdot 10^{-6}$
$R(B \to K^*\mu^+\mu^-)$	34%	29%

Table 12: Rates and branching fractions for the decays $B \to K^*e^+e^-$ and $B \to K^*\mu^+\mu^-$ and $m_t = 150$ GeV.

between the rates for $B \to Kee$ and $B \to K\mu\mu$ is negligible. We also give in Tables 11 and 12 the ratio R for the corresponding exclusive decays, with the inclusive rate for $B \to X_s\, e^+e^-$ and $B \to X_s\, \mu^+\mu^-$ fixed to be:

$$\Gamma(B \to X_s\, e^+e^-) = 7.2 \cdot 10^{-18} \text{ GeV} \quad (75)$$

$$\Gamma(B \to X_s\, \mu^+\mu^-) = 4.1 \cdot 10^{-18} \text{ GeV} \quad (76)$$

We also remark that in estimating the branching ratios in the tables below, if not otherwise stated, we have used the inclusive B decay width

$$\Gamma(B) = 4.84 \times 10^{-13} \text{ GeV} \quad (77)$$

which corresponds to the central value of the present world average of the B hadron lifetime, $\tau_b = 1.36$ ps. The numbers in Tables 11 and 12 are in agreement with other estimates in the literature.

We also remark that the above rates include only the short distance contribution, the importance of including the long distance contributions from the decays $B \to J/\psi(K, K^*) \to \ell^+\ell^-(K, K^*)$, in particular the resulting interference pattern in the invariant mass distributions, is well noted in the literature.

Similarly, we may also use these parametrizations of the Isgur-Wise function to obtain the total rates for the decays $B \to K\ \nu\bar{\nu}$ and $B \to K^*\nu\bar{\nu}$. Integrating the differential distributions yields the rates given in Table 13, for the two parametrizations of the Isgur-Wise function. Again, we give the total rate, the branching fraction and the ratio R for the

	Eq. (73), $w_0 = 1.80$	Eq. (74), $\beta = 0.50$
$\Gamma(B \to K\ \nu\bar{\nu})$ /GeV	$3.1 \cdot 10^{-18}$	$1.4 \cdot 10^{-18}$
$BR(B \to K\ \nu\bar{\nu})$	$6.4 \cdot 10^{-6}$	$2.9 \cdot 10^{-6}$
$R(B \to K\ \nu\bar{\nu})$	8.0%	3.6%
$\Gamma(B \to K^*\ \nu\bar{\nu})$ /GeV	$1.1 \cdot 10^{-17}$	$1.0 \cdot 10^{-17}$
$BR(B \to K^*\ \nu\bar{\nu})$	$2.3 \cdot 10^{-5}$	$2.0 \cdot 10^{-5}$
$R(B \to K^*\ \nu\bar{\nu})$	28.4%	25.8%

Table 13: Rates and branching fractions for the decays $B \to K\ \nu\bar{\nu}$ and $B \to K^*\ \nu\bar{\nu}$, with $m_t = 150$ GeV and summed over three neutrino species.

decay $B \to (K, K^*)\ \nu\bar{\nu}$ summed over three generations. The inclusive rate for $B \to X_s\ \nu\bar{\nu}$ may be obtained from Eq. (42), which for $m_t = 150\ GeV$ is:

$$\Gamma(B \to X_s\ \nu\bar{\nu}) = 3.87 \cdot 10^{-17} \text{ GeV} \quad (78)$$

These processes have relatively large branching fractions and should be measurable at a future asymmetric B factory, if, as remarked already, the decay products of the two B mesons cabn be effectively separated.

4.3 Decay Rates for $(B_s^0, B_d^0) \to \ell^+\ell^-$ and $(B_s^0, B_d^0) \to \gamma\ \gamma$

These decays were discussed some time ago in ref. [28] in the lowest (1 loop) order. With the help of the effective Hamiltonian formalism developed since then it is easy to incorporate the QCD effects, and we refer to a recent calculation of this decay mode in ref. [57]. Neglecting the small corrections, one gets: [3]

$$\Gamma(B_s^0 \to \tau^+\tau^-) = \frac{G_F^2}{\pi}\left(\frac{\alpha}{4\pi}\right)^2 f_{B_s}^2 m_{B_s} m_\tau^2 \sqrt{1 - \frac{4m_\tau^2}{m_{B_s}^2}}\, |V_{tb}V_{ts}^*|^2 |C_9(m_W)|^2 \quad (79)$$

Here f_{B_s} is the B-meson pseudoscalar coupling constant for which we assume $f_{B_s} = 200\ MeV$, and numerically $C_9(m_W) = 3.62$ for $m_t = 150\ GeV$. The branching ratio for $B_s^0 \to \ell^+\ell^-$ can be written as

$$BR(B_s^0 \to \tau^+\tau^-) = 3.8 \times 10^{-7}\left(\frac{f_{B_s}(GeV)}{0.2}\right)^2\left(\frac{|C_9(m_W)|}{3.62}\right)^2 \quad (80)$$

The rates for the decays $B_s^0 \to \mu^+\mu^-$ and $B_s^0 \to e^+e^-$ are suppressed compared to the corresponding rate for $\tau^+\tau^-$ by $(m_\mu/m_\tau)^2$ and $(m_e/m_\tau)^2$, respectively, and they are indeed very small, as can be seen in Table 14. Again, one can express the decay rates $\Gamma(B_d^0 \to \ell^+\ell^-)$ in terms of the rates for $\Gamma(B_s^0 \to \ell^+\ell^-)$ using the relation in the CKM model:

$$\frac{\Gamma(B_d^0 \to \ell^+\ell^-)}{\Gamma(B_s^0 \to \ell^+\ell^-)} = \frac{|V_{td}|^2}{|V_{ts}|^2}(1 + \delta_\ell), \quad (81)$$

[3] Note that there is a factor of 2 missing in the expression for the decay rate given in ref. [4] and [28]. We thank Andrzej Buras for drawing our attention to it.

with δ_ℓ is again an $SU(3)$-breaking parameter. Again, for the default value $|V_{td}/V_{cb}| = 0.21$ one expects the branching ratios for $B_d^0 \to \ell^+\ell^-$ to be suppressed by ~ 22, as compared to the corresponding decays $B_s^0 \to \ell^+\ell^-$. We have listed these branching ratios in Table 14 for $m_t = 150$ GeV, dropping δ_ℓ.

Finally, the branching ratio for the process $B_s^0 \to \gamma\,\gamma$ is:

$$BR(B_s^0 \to \gamma\gamma) = 1.5 \times 10^{-8} \left(\frac{f_{B_s}(GeV)}{0.2}\right)^2 \left(\frac{|I^+(m_t)|}{0.43}\right)^2 \qquad (82)$$

where the function $I^+(m_t)$ is given in ref. [28]. The branching ratio for this and the corresponding one involving the CKM-suppressed decay $BR(B_d^0 \to \gamma\gamma)$ are listed in Table 14 with $m_t = 150$ GeV.

Decay Modes	Br	Experimental Upper Limits (90 % C.L.)
$(B_d, B_u) \to X_s\gamma$	3.5×10^{-4}	8.4×10^{-4} [CLEO][56]
$(B_d, B_u) \to K^*\gamma$	$(4.0 - 6.8) \times 10^{-5}$	0.92×10^{-4} [CLEO][56]
$(B_d, B_u) \to X_d\gamma$	1.5×10^{-5}	–
$(B_d, B_u) \to \rho + \gamma$	$(2.8 - 4.5) \times 10^{-6}$	–
$(B_d, B_u) \to X_s e^+e^-$	1.5×10^{-5}	–
$(B_d, B_u) \to X_d e^+e^-$	6.5×10^{-7}	–
$(B_d, B_u) \to X_s \mu^+\mu^-$	8.5×10^{-6}	5.0×10^{-5} [UA1][45]
$(B_d, B_u) \to X_d \mu^+\mu^-$	3.7×10^{-7}	–
$(B_d, B_u) \to K e^+e^-$	6.0×10^{-7}	5.0×10^{-5} [PDG][18]
$(B_d, B_u) \to K \mu^+\mu^-$	6.0×10^{-7}	1.5×10^{-4} [PDG][18]
$(B_d, B_u) \to K^* e^+e^-$	5.6×10^{-6}	–
$(B_d, B_u) \to K^* \mu^+\mu^-$	2.9×10^{-6}	2.3×10^{-5} [UA1][45]
$(B_d, B_u) \to X_s\,\nu\bar{\nu}$	8.0×10^{-5}	–
$(B_d, B_u) \to X_d\,\nu\bar{\nu}$	3.5×10^{-6}	–
$(B_d, B_u) \to K\,\nu\bar{\nu}$	6.4×10^{-6}	–
$(B_d, B_u) \to K^*\,\nu\bar{\nu}$	2.3×10^{-5}	–
$B_s \to \gamma\gamma$	1.5×10^{-8}	–
$B_d \to \gamma\gamma$	6.5×10^{-10}	–
$B_s \to \tau^+\tau^-$	3.8×10^{-7}	–
$B_d \to \tau^+\tau^-$	1.7×10^{-8}	–
$B_s \to \mu^+\mu^-$	1.8×10^{-9}	–
$B_d \to \mu^+\mu^-$	8.0×10^{-11}	–
$B_s \to e^+e^-$	4.2×10^{-14}	–
$B_d \to e^+e^-$	1.9×10^{-15}	–

Table 14: Estimates of the branching fractions for FCNC B-decays in the Standard Model for $m_t = 150\ GeV$, $\mu = 5\ GeV$ and $f_{B_d} = 200\ MeV$. Note that the CKM-suppressed decays depend quadratically on $|V_{td}|$, and the numbers correspond to $|V_{td}| = 9.18 \times 10^{-3}$. Experimental upper limits are also listed.

5 OVERVIEW and OUTLOOK

Theoretical interest in rare B-decays lies in the first place in their potential role as precision tests of the Standard Model in the flavour sector. Within the Standard Model, their eventual measurements will provide quantitative information about the top quark mass and more importantly about the CKM matrix-elements, V_{td}, V_{ts} and V_{tb}. In particular, the CKM-suppressed rare B-decays directly measure V_{td}. Together with improved measurements of the CKM matrix elements $|V_{cb}|$ and $|V_{ub}|$, the measurements of $|V_{td}|$ will determine the CKM unitarity triangle, pinning down the CP violating phases in the Standard Model. However, rare B-decay may provide one of the early hints for the non-SM physics. It is, therefore, imperative to get as reliable estimates of these decays in the SM as possible.

We have discussed in this report a number of inclusive and exclusive branching ratios and distributions involving rare B-decays in the Standard Model. The estimates presented here are based on the applications of QCD, whose role lies in both sharpening the theoretical expectations and in providing a dependable energy-momentum profile of the final states. Based on the successful applications of perturbative QCD in studies of the inclusive CC semileptonic and non-leptonic B-decays, one expects that applications of the same in inclusive FCNC B-decays will also provide reliable estimates. However, they remain to be tested experimentally.

We emphasize that it would be worthwhile to measure the hard photon energy spectra in the inclusive B-decays, $B \to X + \gamma$. Photons from the CC B decays $B \to (X_c, X_u) + \gamma$ are interesting in their own right providing a detailed test of the dynamics of hard photon emission in heavy meson decays. These photons range out by ~ 2 GeV from B decays at rest due to kinematics, or else they are emitted at a reduced rate due to the CKM suppression in the decays $B \to X_d + \gamma$. Hence, photons with $E_\gamma \geq 2GeV$ in B decays are likely candidates for the FCNC processes $B \to (X_s, X_d) + \gamma$. In principle, one could distinguish the CKM-allowed and -suppressed rare B-decays by flavour-tagging the hadrons in X_s, which should have an overall strangeness quantum number $S = -1$, and in X_d, consisting of light hadrons with an overall $S = 0$. In view of this, we emphasize good photon measurement capability to study a large class of very interesting B decays involving photonic transitions.

While the radiative rare B-decays are expected to have larger branching ratios, and hence emphasized quite a bit here, the FCNC B-decays involving dileptons are equally promising, since they can be searched for in hadron collisions also, such as at the Fermilab Tevatron, LHC, and SSC, and in fixed target dedicated B physics facilities. With an estimated yield of $O(10^9 - 10^{12})$ B-hadrons at these facilities, many of the inclusive and exclusive dilepton decay modes are detectable. In fact, the present best limits on their seraches have been obtained from the $p\bar{p}$ colliders at CERN and Fermilab.

The FCNC semileptonic and purely leptonic B decays can be classified as the CKM-allowed and CKM-suppressed transitions involving the matrix element V_{ts} and V_{td}, respectively. Their rates and various dilepton distributions are sensitive to both m_t and non-SM interactions. We have worked out the m_t-dependence in many examples in this report. Experiements searching for CP violation in B decays, based on $B \to J/\psi + K_s$, have a built-in sensitivity for measuring FCNC semileptonic and leptonic decays, such as $B \to X_s\ell^+\ell^-$, with the dilepton mass being different from the J/ψ and ψ' masses to reduce the CC component.

Theoretical predictivity in exclusive rare B-decays is less sharp. This is so since rare

B-decays involve the so-called heavy to light hadron transitions, as opposed to the heavy to heavy CC decays $B \to (D, D^*)\ell\nu_\ell$, which have been quantitatively studied in the HQET framework and are under theoretical control. Significantly firm statements on the exclusive rare B-decays can be made if the CKM-suppressed CC exclusive decays become available experimentally. They will allow measurement of the Isgur-Wise function over a large kinematic region, reducing the parametrization dependence, but to be able to predict quantitatively the rates, one will have to estimate power corrections. From an experimental point of view, however, exclusive rare B-decay searches, such as $B \to K^* + \gamma$, $B \to \rho + \gamma$, and $B \to (K, K^*, \pi, \rho)\ \ell^+\ell^-$, are easier given enough statistics. In view of the ongoing seraches, we reviewed estimates of some exclusive decays. They were based in part on vector meson dominance approximation, which we consider experimantally verified in low invariant mass sytems and hence also useful in similar kinematic domains in rare B decays, and in part on the HQET-motivated models. Clearly, there is lot of room for improvement here and we hope that the quantitative study of FCNC exclusive decays will receive the theoretical attention it deserves. Despite this, and with the imminent discovery of the penguin dominated decay mode $B \to K^* + \gamma$ around the corner, we would like to stress that a branching ratio $(4.0 - 7.0) \times 10^{-5}$ is a fairly confident prediction of the Standard Model for this decay mode.

The full potential of FCNC B physics will be realized only in dedicated B physics experiments, such as at a B factory and in future hadronic collisions. The ultimate prize in B physics is to get a deeper understanding of CP violation, but along the way there are also other precious discoveries to be made. We have given a profile of FCNC B decays where many of such discoveries are in store, some of them almost at the level of the present experimental sensitivity.

References

[1] S.L. Glashow, Nucl. Phys. **22** (1961) 579; S. Weinberg, Phys. Rev. Lett. **19** (1967) 1264; A. Salam, in *Elementary Particle Theory*, Editor: N. Svartholm (Almqvist and Wiksell) (1968).

[2] S.L. Glashow, J. Illiopoulos, and L. Maiani, Phys. Rev. **D2** (1970) 1285.

[3] N. Cabibbo, Phys. Rev. Lett. **10** (1963) 531;
M. Kobayashi and K. Maskawa, Prog. Theor. Phys. **49** (1973) 652.

[4] A. Ali, DESY Report 12-058 (1992) and in *Proceedings of the 1991 Summer School in High Energy Physics and Cosmology, ICTP, Trieste;* Editors: E. Gava et al. (World Scientific) (1992).

[5] S. Bertolini, SISSA Reports 142/92/EP and 188/92/EP (1992).

[6] H. Schröder, in *QCD-20 Years Later*, Aachen, June 9-13, 1992.

[7] A. Ali and D. London, DESY Report 92-075 (1992) (to appear in J. Phys. G, UK), and in these proceedings.

[8] L. Wolfenstein, Phys. Rev. Lett. **51** (1983) 1945.

[9] S. Bertolini, F. Borzumati and A. Masiero, Phys. Rev. Lett. **59** (1987) 180;
R. Grigjanis et al., Phys. Lett. **B213**(1988) 355;
M. Misiak, Phys. Lett. **B269** (1991) 161.

[10] B. Grinstein, M.J. Savage, M.B. Wise, Nucl. Phys. **B319** (1989) 271.

[11] B. Grinstein, R. Springer and M. B. Wise, Nucl. Phys. **B339** (1990) 269.

[12] G. Cella et al., Phys. Lett. **B248** (1990) 181.

[13] A. Ali and C. Greub , Z. Phys. **C49** (1991) 431; Phys. Lett. **B259** (1991) 182.

[14] A. Ali and C. Greub , Phys. Lett. **B287** (1992) 191.

[15] A. Ali and C. Greub , Phys. Lett. **B293** (1992) 226.

[16] A. Ali and E. Pietarinen, Nucl. Phys. **B154** (1979) 519.

[17] G. Altarelli et al., Nucl. Phys. **B208** (1982) 365.

[18] K. Hikasa et. al. (Particle Data Group), Phys. Rev. **D45** (1992) 1.

[19] N. Isgur and M. Wise, Phys. Lett. **B232** (1989) 113; *ibid.* **B237** (1990) 527.

[20] see, e.g., T. Mannel, *Heavy Quark Effective Theory: Applications to B Decays*, these proceedings.

[21] N. Isgur and M. Wise, Phys. Rev. **D42** (1990) 2388.

[22] G. Burdman, J.F. Donoghue, Phys. Lett. **B270** (1991) 55.

[23] C.S. Lim, T. Morozumi and A.I. Sanda, Phys. Lett. **B218** (1989) 343.

[24] A. Ali, T. Mannel and T. Morozumi, Phys. Lett. **B273** (1991) 505.

[25] A. Ali and T. Mannel, Phys. Lett. **B264** (1991) 447. Erratum: *ibid* **B274** (1992) 526.

[26] A. Ali, T. Ohl and T. Mannel, Phys. Lett. **B298** (1993) 195.

[27] A. Ali, T. Feldmann and T. Mannel (in preparation).

[28] B.A. Campbell and P.J.O'Donnell, Phys. Rev. **D25** (1982) 1989.

[29] T. Inami and C.S. Lim, Progr. Theor. Phys. **65** (1981) 297.

[30] G. Altarelli and S. Petrarca, Phys. Lett. **B261** (1991) 303.

[31] A. Paschos and U. Türke, Phys. Rep. **178** (1989) 145.

[32] J. Carter, Proceedings of the *International Lepton-Photon Symposium and Europhysics Conference on High Eneregy Physics*, S. Hegerty, K. Potter and E. Quercigh eds. (Geneva, 1991).

[33] G. Altarelli, in *QCD-20 Years Later*, Aachen, June 9-13, 1992.

[34] A. J. Buras and M.K. Harlander, MPI-PAE/PTh 1/92; TUM-T31-25/92 (1992).

[35] G. Eigen (CLEO), DESY Seminar, June 23, 1992.

[36] A.J. Buras, W. Słominski and H. Steger, Nucl. Phys. **B238** (1984) 529; **B245** (1984) 369.

[37] J. Flynn, Mod. Phys. Lett. **A5** (1990) 877.

[38] A.J. Buras, M. Jamin, and P.H. Weisz, Nucl. Phys. **B347** (1990) 491.

[39] M. Lusignoli et al., Nucl. Phys. **B369** (1992) 139;
C. Alexandrou et al., Nucl. Phys. **B374** (1992) 263.

[40] P.S. Drell and J. Ritchie Patterson, Cornell University Report CLNS-92-1177 (1992) (to appear in Proceedings of the 26th. International Conference on High Eneregy Physics, Dallas, Texas, USA, (1992)).

[41] R. Fulton et al. (CLEO), Phys. Rev. Lett. **64** (1990) 16; S. Stone (Private communication).

[42] H. Albrecht et al. (ARGUS), Phys. Lett. **B234** (1990) 409; *ibid* **B249** (1990) 359.

[43] M. Battle et al. (CLEO), contributed paper to the *Joint Inter. Lepton Photon Symp. and Europhys. Conf. on High Energy Physics*, Geneva (1991).

[44] G. Eilam, R.Mendel and R. Migneron, Z. Phys. **C52** (1991) 145.

[45] C. Albajar et al. (UA1), Phys. Lett. **B262** (1991) 163.

[46] P.J. O'Donnell and H.K.K. Tung , Phys. Rev. **D43** (1991) R2067;
N. Paver and Riazuddin, Phys. Rev. **D45** (1992) 978.

[47] W. Hou, R. Willey and A. Soni, Phys. Rev. Lett. **58** (1987) 1608.

[48] W. Buchmüller and D. Wyler, Phys. Lett. **B 177** (1986) 377;
B.A. Campbell et al., Int. J. Mod. Phys. **A2** (1987) 831.

[49] A. Falk, Nucl. Phys. **B378** (1992) 79.

[50] B. Grinstein, N. Isgur, D. Scora, and M. Wise, Phys. Rev. **D39** (1989) 799.

[51] G.W. Brandenburg et al., Phys. Rev. Lett. **36** (1976) 703;
R.K. Carnegie et al., Phys. Lett. **B68** (1977) 287;
D.G.W.S. Leith, in *Proc. 5th Intl. Conf. on Experimental Meson Spectroscopy*, Eds. E. von Goeler and R. Weinstein, Northeastern University Press, Boston, 1977.

[52] N. Deshpande, P. Lo, and J. Trampetic, Phys. Rev. Lett. **59** (1987) 183.

[53] T. Altomari, Phys. Rev. **D37** (1988) 677.

[54] T. Hayashi, M. Matsuda, and M. Tanimoto, Kogakkan Univ. Report KU-01-93 (1993).

[55] N. Isgur and M. Wise, Phys. Rev. **D41** (1990) 151, Phys. Rev. **D42** (1990) 2388.

[56] E.H. Thorndike (CLEO Collaboration), Contributed paper # 531, LP-HEP 91 Conference, Geneva, Switzerland.

[57] A.J. Buras and G. Buchalla, Max-Planck Institute Report MPI-PTh-2-93 (1993).